

Modeling 1993–2008 climatology of seasonal general circulation and thermal structure in the Great Lakes using FVCOM

Xuezhi Bai ^{a,*}, Jia Wang ^b, David J. Schwab ^b, Yi Yang ^{a,c}, Lin Luo ^a, George A. Leshkevich ^b, Songzhi Liu ^a

^a Cooperative Institute for Limnology and Ecosystems Research, University of Michigan, 4840 S. State Road, Ann Arbor, MI 48108, USA

^b NOAA Great Lakes Environmental Research Laboratory, 4840 S. State Road, Ann Arbor, MI 48108, USA

^c Hainan Marine Development Plan and Design Institute, Haikou, Hainan, China

ARTICLE INFO

Article history:

Received 6 September 2012

Received in revised form 5 February 2013

Accepted 9 February 2013

Available online 6 March 2013

Keywords:

Great Lakes
General circulation
Thermal structure
Modeling
FVCOM

ABSTRACT

An unstructured Finite Volume Coastal Ocean Model was applied to all five Great Lakes simultaneously to simulate circulation and thermal structure from 1993 to 2008. Model results are compared to available observations of currents and temperature and previous modeling work. Maps of climatological circulation for all five Great lakes are presented. Winter currents show a two-gyre type circulation in Lakes Ontario and Erie and one large-scale cyclonic circulation in Lakes Michigan, Huron, and Superior. During the summer, a cyclonic circulation remains in Lakes Superior; a primarily cyclonic circulation dominates upper and central Lake Huron; Lake Ontario has a single cyclonic circulation, while circulation in the central basin of Lake Erie remains two-gyre type; Lake Michigan has a cyclonic gyre in the north and an anti-cyclonic one in the south. The temperature profile during the summer is well simulated when a surface wind-wave mixing scheme is included in the model. Main features of the seasonal evolution of water temperature, such as inverse temperature stratification during the winter, the spring and autumn overturn, the thermal bar, and the stratification during summer are well reproduced. The lakes exhibit significant annual and interannual variations in current speed and temperature.

© 2013 Elsevier Ltd. All rights reserved.

1. Introduction

Hydrodynamic processes and thermal structure in the Great Lakes directly affect the chemical, biological, and ecological dynamics of the system. Horizontal and vertical transport and mixing influence the distribution of nutrients, contaminants, and biota (Schwab, 1992). Changes in the temperature field can change the volume of the optimal thermal habitats of fish species and result in permanent changes in the fish community and in fish production (Hill and Magnuson, 1990). Due to the size of the Great Lakes, it is very difficult to collect extensive synoptic field data in a short period. Therefore, mathematical and physical models play important roles in the integration and interpretation of field data and in extending the understanding of the nature of water circulation in the Great Lakes.

There have been many efforts to model the Great Lakes since the 1970s. The models have developed from linear, vertically integrated, steady-state models (Rao and Murty, 1970; Simons, 1971) to state of the art comprehensive three-dimensional hydrodynamic models. Lake Michigan's large-scale circulation has probably been studied most extensively. Beletsky and Schwab (2001) and Beletsky et al. (2006, 2008) simulated multi-year general circulation

and thermal structure in Lake Michigan using Princeton Ocean Model, studied the annual cycle and interannual variability, and obtained the climatological circulation pattern in Lake Michigan. Recently, models have been developed for other Great Lakes. Zhu et al. (2001) and Chen et al. (2001) developed a hydrodynamic model to study the development of the currents along the Keweenaw Peninsula and the effects of heat fluxes on the coastal jet intensification. Bennington et al. (2010) simulated Lake Superior's general circulation and thermal structure from 1979 to 2006 using the MIT general ocean model. They further studied the interannual variability and the long-term trend. Sheng and Rao (2006) simulated the circulation of Lake Huron for 1974–1975 using a high resolution, nested grid hydrodynamic model and presented monthly mean circulation and thermal structure of the lake. Schwab et al. (2009) present simulated summer currents in Lake Erie for 1994, and Prakash et al. (2007) used a hydrodynamic model to simulate mean circulation patterns and pollutant transport in Lake Ontario. For the first time in the Great Lakes, Wang et al. (2010) employed a CIOM (Coupled Ice-Ocean Model) to simulate ice cover in Lake Erie.

NOAA's operational Great Lakes Coastal Forecasting system (GLCFS) (Schwab and Bedford, 1999) uses a POM to simulate the daily circulation and temperature for each of the Great Lakes <http://www.glerl.noaa.gov//res/glcfs/>.

Each of these models has been applied to a single Great Lake. These models are important in understanding the mean

* Corresponding author. Tel.: +1 734 741 2247.

E-mail addresses: xuezhi.bai@noaa.gov, xuezhi@umich.edu (X. Bai).

circulation, thermal structure, and coastal processes; however, for the studies of climate response in the context of the whole watershed of the Great Lakes, a basin-scale five-lake hydrodynamic model is needed. A five-lake model can be more easily coupled to a regional climate model, hydrological model, or lake ice model. Because of significant differences in shape and depth, the responses to a same climatic forcing may be different in each lake. This multi-lake model would also be a useful tool to understand the different responses of each lake. Furthermore, reliable information on long-term circulation patterns in the Great Lakes is sorely needed for a variety of issues ranging from water quality predictions to sediment transport and ecosystem modeling (Beletsky and Schwab, 2008; Luo et al., 2012). For the first time, Beletsky and Schwab (2008) constructed maps of the climatological circulation in Lake Michigan based on 10 continuous years of model output (1998–2007). Recently, Bennington et al. (2010) presented climatological circulation maps for Lake Superior based on 1979–2006 model outputs. Up to now, we still do not have a map of climatological circulation based on modeling for the whole Great Lakes.

The previous models for the Great Lakes (e.g. Beletsky et al., 2006) usually produce a too-shallow mixed layer, and a too-diffusive thermocline during the summer, compared to the observations. One major reason is that the wind-wave mixing effect is not included. Craig and Banner (1994) considered the effect of wave breaking on mixing. However, their model does deepen the mixed layer in a one-dimension calculation, but has a relatively small influence on the three-dimension calculation (Mellor and Blumberg, 2004). Qiao et al. (2004) used a spectral wave model (Yuan et al., 1991) to derive wave-induced mixing on the basis of a linear wave theory (Yuan et al., 1999) and found that adding wave-induced mixing to the vertical diffusivity in a global ocean circulation model yields a temperature structure closer to the observation. On the basis of the same theory as Yuan et al. (1999) and Qiao et al. (2004), Hu and Wang (2010) developed a wind-wave mixing scheme by using a single typical linear wave to represent the wave spectrum. During the setup of the 5-lakes model, we attempt to improve the model's accuracy in reproducing

the upper layer thermal structure in the Great Lakes by incorporating Hu and Wang (2010) simple and practical scheme into the multi-lake model.

In this paper, we simulate the circulation and thermal structure of the five Great Lakes from 1993 to 2008, using an unstructured Finite Volume Coastal Ocean Model (FVCOM, with no ice component). Modeled currents and temperatures are compared to available observations and previous modeling work as well. Seasonal maps of the climatological circulation are constructed for all five Great Lakes based on 15 years of continuous modeling. We describe the success and limitations of modeled results, especially the circulation. We discuss the main features of the seasonal evolution of water temperature in the Great Lakes. The annual and interannual variations in current speed and water temperature are examined.

2. Model

The GL-FVCOM (Great Lakes Finite Volume Coastal Ocean Model) is a spherical coordinate version of the unstructured-grid finite-volume, three-dimensional primitive equation coastal ocean model developed originally by Chen et al. (2003) and upgraded by the UMASS-D/WHOI model development team (Chen et al., 2006). The FVCOM uses an unstructured triangular mesh in the horizontal, which well represents the complex geometry. FVCOM uses the modified Mellor and Yamada level 2.5b (MY-2.5) and Smagorinsky turbulent closure schemes as default setups for vertical and horizontal mixing, respectively (Mellor and Yamada, 1982; Mellor, 2001; Mellor and Blumberg, 2004; Smagorinsky, 1963). FVCOM is numerically solved using a split-mode method.

The computational domain of GL-FVCOM covers the entire Great Lakes (Fig. 1).

Lakes Michigan and Huron were connected, while the other lakes were kept disconnected due to the nature of their connection (straits between Michigan and Huron, rivers between the others). The unstructured triangular grid has an average horizontal resolution of about 3.5 km (Fig. 2). The GL-FVCOM has 21 terrain

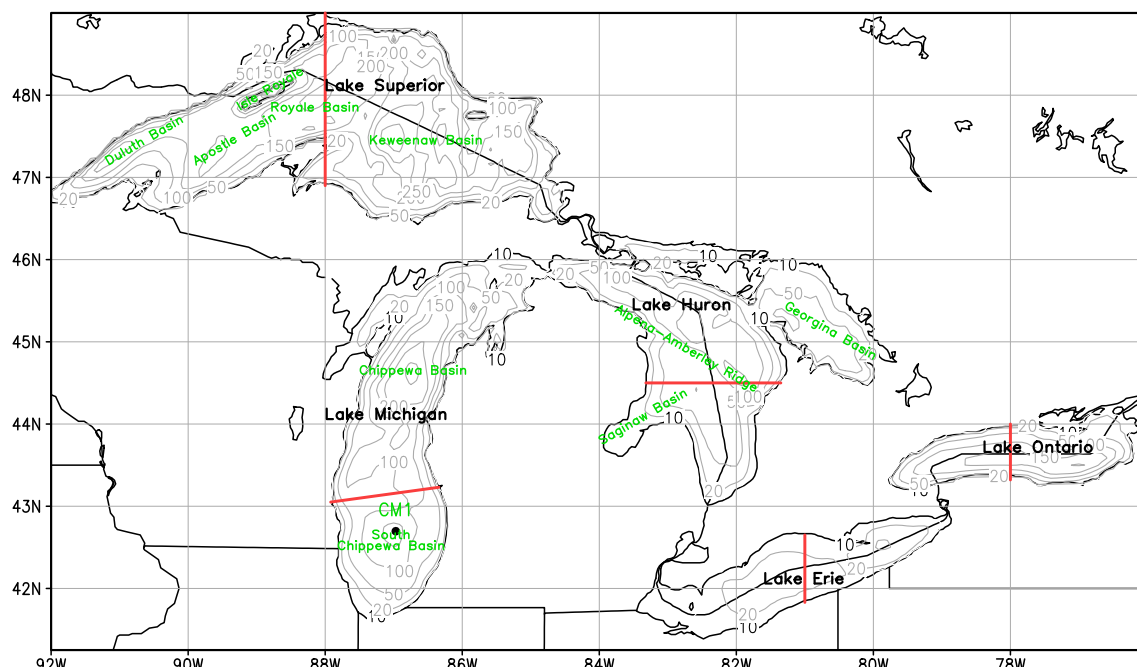


Fig. 1. The Great Lakes basin regional bathymetry map. CM1 denotes a mooring site in southern Lake Michigan. The red solid lines denote transects in the five lakes.

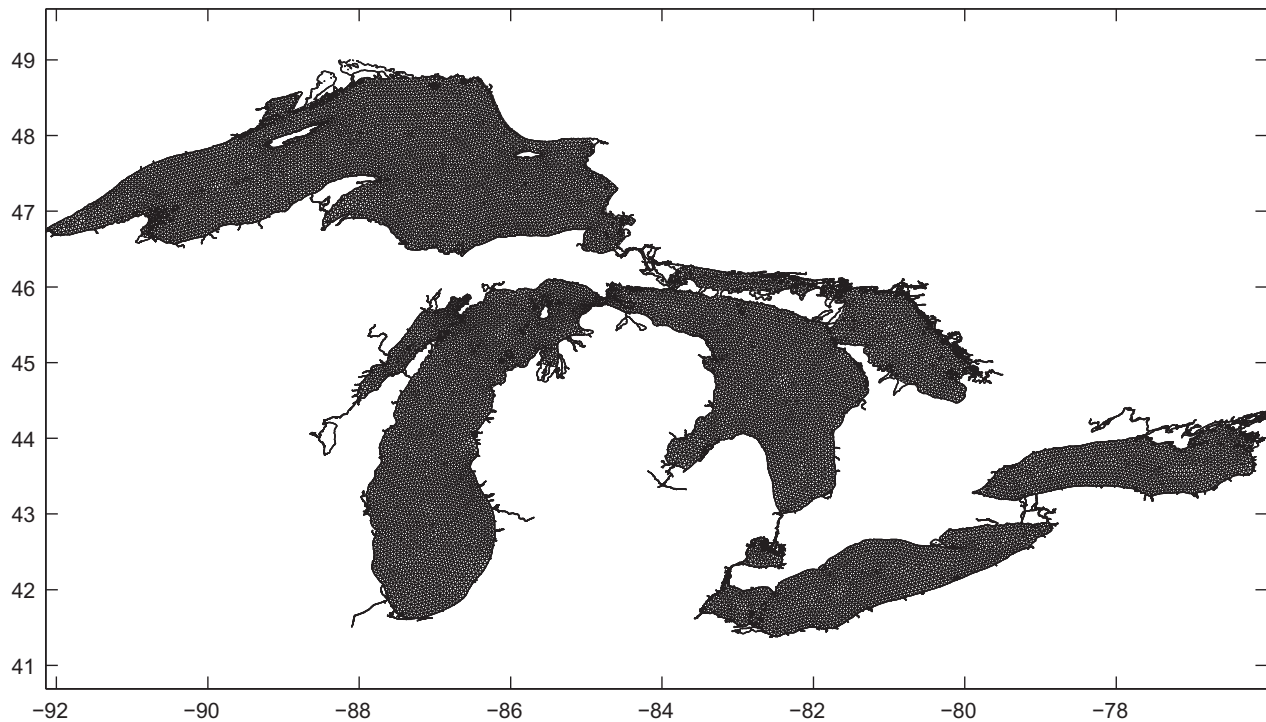


Fig. 2. Unstructured grid of the model.

following vertical layers with higher resolution near the surface and bottom to better resolve the mixing processes.

The model is forced with 3-hourly surface winds, air temperature, net downward shortwave radiation at the surface, total cloud cover, and specific humidity from the North American Regional Reanalysis (NARR) (Mesinger et al., 2006) between 1993 and 2008. This forcing has a uniform horizontal resolution of 32 km.

The incoming shortwave radiation can penetrate beyond the surface layer and passively heat water at depth. To specify the short wave radiation, the model uses the classification of Jerlov (1968, 1976) as interpreted by Paulson and Simpson (1977). The long-wave radiation is calculated as a function of air temperature, model surface temperature, and cloud cover according to Wyrtki (1965). We use a bulk aerodynamic formulation to calculate latent and sensible heat fluxes over the water surface at each grid point for the model. The transfer coefficients are calculated considering the appropriate stability parameter according to the bulk aerodynamic method suggested by Large and Pond (1982).

A surface wind-wave mixing scheme, developed by Hu and Wang (2010) based on the same wave-induced mixing theory as Yuan et al. (1999) and Qiao et al. (2004), was included in the model. The surface wind-wave mixing is parameterized into the model:

$$K_{mw} = \frac{2v^2}{g} \delta \beta^3 W^3 e^{\frac{gz}{\delta^2 w^2}} \quad (1)$$

where K_{mw} is the wind-wave induced vertical kinematic viscosity coefficient; β is the wave age ($0 < \beta < 1$ for growing wave, and $\beta = 1$ for mature wave), δ is the wave steepness ($\delta = 2\alpha/\lambda$, α is the amplitude and λ is the wavelength), W is the wind speed, $z < 0$ is the depth, $v = 0.4$ is the von Karman constant, and g is acceleration due to gravity. In this study, we set $\beta = 0.5$ and $\delta = 0.16$. Surface wind-wave reduced vertical diffusivity coefficient K_{hw} is assumed equal to K_{mw} .

The total mixing coefficient is the sum of wind-wave induced $K_{mw}(K_{hw})$ and $K_m(K_h)$, which is calculated by the level 2.5 closure

turbulence model. K_m and K_h are vertical kinematic viscosity and vertical diffusivity, respectively.

The minimum depth was set to 10 m. Based on the Courant–Friedrichs–Lowy (CFL) criterion, the internal mode time step of the integration is 300 s, while the external mode time step is 15 s. The model runs from January 1, 1993 through December 31, 2008 with an initial temperature of 2 °C and motionless state. As we do not have an ice model, the surface temperatures in the model are set to zero when the surface temperature drops to below zero during winter. Ice effects on surface wind friction are not considered in the model.

3. Data

Temperature data from satellites and moorings, and current data from moorings is used to evaluate the model simulation.

Drift bottle and drift card have been used to study the currents in the Great Lakes since the late 19th century (Harrington, 1895). The Federal Water Pollution Control Administration conducted the earliest direct open-lake currents measurements in the early 1960s. The current meters and temperature recorders were placed on numerous moorings throughout the lakes. The moorings consisted of a series of current meters placed on a taut line suspended in the water column beneath subsurface floats. The earliest current measurements were made with early models of self-contained Savonius rotor meters that recorded data on photographic film. More recently, currents have been measured with arrays of vector-averaging current meters, which record the east and north components of the current flow past the meter for selected fixed intervals of time (Beletsky et al., 1999b). Many circulation experiments were performed in the Great Lakes since the 1960s. The experiments usually lasted for one year covering the whole seasonal cycle, though some of them were shorter or longer (see Table 1 in Beletsky et al., 1999b). Based on the measurements, many researchers reported monthly or seasonal mean circulations in different depths for all the individual lakes. Beletsky et al.

Table 1

Seasonal and annual mean current speed and standard deviation derived from daily mean current speed and standard deviation (unit: cm/s).

	Superior	Michigan	Huron	Erie	Ontario	GLS
Winter	2.92 ± 0.95	3.10 ± 0.81	2.83 ± 0.84	2.55 ± 0.92	2.23 ± 0.83	2.46 ± 0.64
Summer	1.67 ± 0.56	2.17 ± 0.52	1.82 ± 0.43	1.92 ± 0.55	1.61 ± 0.45	1.70 ± 0.33
Annual	2.34 ± 0.79	2.70 ± 0.69	2.41 ± 0.66	2.31 ± 0.79	1.90 ± 0.61	2.12 ± 0.50

(1999b) presented maps of mean circulation in the Great Lakes, employing long-term current observations from about 100 Great Lakes moorings during the 1960s to 1980s. We use these studies rather than the raw data as references to validate the modeled general circulation.

The Great Lakes Surface Environmental Analysis (GLSEA) is a digital map of the lake surface temperatures and ice cover, which is produced daily from the satellite Advanced Very High Resolution Radiometer (AVHRR) instrument at NOAA's Great Lakes Environmental Research Laboratory (GLERL) (Schwab et al., 1992). The data are available from 1994 to present. The AVHRR data were mapped into a Mercator projection and re-sampled to a 512×512 pixel grid covering the area $38.89\text{--}50.58^\circ\text{N}$, $75.88\text{--}92.41^\circ\text{W}$ with the pixel size of 2.56 km in mid-latitude (Table 1 in Schwab et al., 1992). The daily average GLSEA surface water temperature data for each lake from 1994 to 2008 were obtained from the GLERL Coastwatch program (<http://coastwatch.glerl.noaa.gov/statistic/statistic.html>).

Moored thermistor strings continually measure water temperatures at varying depths, which provides site specific subsurface data to validate the model's vertical thermal structure. Started in April 1990, a site called CM1 was established in southern Lake Michigan to measure the vertical thermal structure. A subsurface mooring contains an 80 m long thermistor chain moored to cover depths from approximately 20–100 m (McCormick and Pazdalski, 1993). In this paper, we use data for 1998 to validate the model's thermal structure. During 1998, the thermistors were located at the following depths: 17, 27, 32, 37, 47, 77, 87, 97, 107, and 152 m. The daily temperatures at depths were obtained from 1 h interval temperature data.

To measure the skill for reproducing the measurements, two statistical measures are introduced to conduct the model-data comparison. Mean bias deviation (MBD) is defined as

$$\text{MBD} = 100 \frac{\frac{1}{N} \sum_{i=1}^N (x_i - y_i)}{\frac{1}{N} \sum_{i=1}^N y_i} = 100 \frac{\bar{x} - \bar{y}}{\bar{y}} \quad (2)$$

and root mean square error (RMSE) is defined as

$$\text{RMSE} = \sqrt{\frac{1}{N} \sum_{i=1}^N (x_i - y_i)^2} \quad (3)$$

where x_i and y_i ($i = 1, 2, 3, \dots, N$) are the modeled and observed time series of any variable such as surface temperature, water currents etc. N is the total sampling number, and the over bars denote the average of the time series. MBD directly measures the relative bias or error of the modeled time series from the observed in percentage. RMSE measures the absolute error of the modeled time series against observation.

4. General circulation

In this section, we present the model's long-term seasonal mean circulation, which is validated against the observations and compared with the previous model's results. We choose DJFM (December–March) mean for winter and JJAS (June–September) for summer. Seasonal mean surface winds for winter and summer averaged over the simulation period from 1993 to 2008 (Fig. 3) show westerly prevailing winds over Lakes Michigan, Huron, Erie,

and Ontario, and northwesterly winds over Lake Superior during winter. Southerly or southwesterly winds prevail over the Great Lakes during summer.

The long-term mean (1973–2010) Annual Maximum Ice Coverage (AMIC) for the five lakes are 63.3% for Lake Superior, 38.6% for Lake Michigan, 62.7% for Lake Huron, 83.7% for Lake Erie, and 26.8% for Lake Ontario (Bai et al., 2011). Lakes Michigan and Ontario usually do not have an extensive ice cover. During the simulated period (1993–2011), the AMICs for the two lakes in most years are only 10–20% (Bai et al., 2012). Thus, the effects of ice cover on the simulated winter circulation in Lakes Michigan and Ontario are not as significant as other heavily ice-covered lakes.

4.1. Winter isothermal period

During the winter, surface cooling produces nearly isothermal water, so that with only weak density gradients, currents would be primarily wind-driven (Pickett, 1980). Fig. 4 shows depth-averaged currents from the model averaged during the winters of 1994–2008. Winter currents are essentially barotropic because of the little horizontal density gradients. There is one large cyclonic circulation in the larger lakes (Lakes Michigan, Huron, and Superior) and a two-gyre type wind-driven circulation in smaller lakes (Lakes Ontario and Erie). The cyclonic circulation in the larger lakes is mainly attributed to the regional lake-induced cyclonic vorticity in the atmosphere (Pettersen and Calabrese 1959; Beletsky et al., 1999a; Schwab and Beletsky, 2003). Topographic effects are also important but are not as significant as wind stress curl (Schwab and Beletsky, 2003). Winter circulation in Lake Ontario and in Lake Erie strongly resembles the classic two-gyre wind-driven circulation (Rao and Murty, 1970; Bennett, 1974). Due to the orientation (parallel to the dominate westerly winds) and small size, the wind stress curl over Lakes Erie and Ontario is small. The Rao and Murty studies showed that, in lakes with sloping bottoms, the large-scale steady state circulation pattern due to a uniform wind stress generally consists of a pair of counter-rotating gyres with downwind flow near the shores and upwind return flow in the deeper parts of the basin (Schwab and Beletsky, 2003). This pattern is independent of both stratification and rotation (Bennett, 1974).

4.1.1. Lake Superior

The modeled winter mean currents in Lake Superior show a basin-scale cyclonic circulation with strong coastal currents (Fig. 5(a)). The currents in the far west end of the lake are much weaker than other areas, which are less than 1 cm/s, however the observations during the 1966–1967 winter showed much stronger currents (Sloss and Saylor, 1976; Beletsky et al., 1999b) (Fig. 5(b)). The northern coastal flow diverges into two branches when it reaches Isle Royale (see Fig. 1): the northern branch flows southwestward until northeast of the Duluth Basin, where it flows southward to join the strong southern coastal currents; the south branch flows southwestward until the ridge between the Royale Basin and the Apostle Basin where most parts of it flow southward to join the southern coastal currents. The strongest currents are east of the Keweenaw Peninsula. The large cyclonic circulation consists of four cyclonic gyres in the eastern end, and in the Keweenaw, Royale, and Apostle basins. Topographic effect is the primary cause of these four gyres.

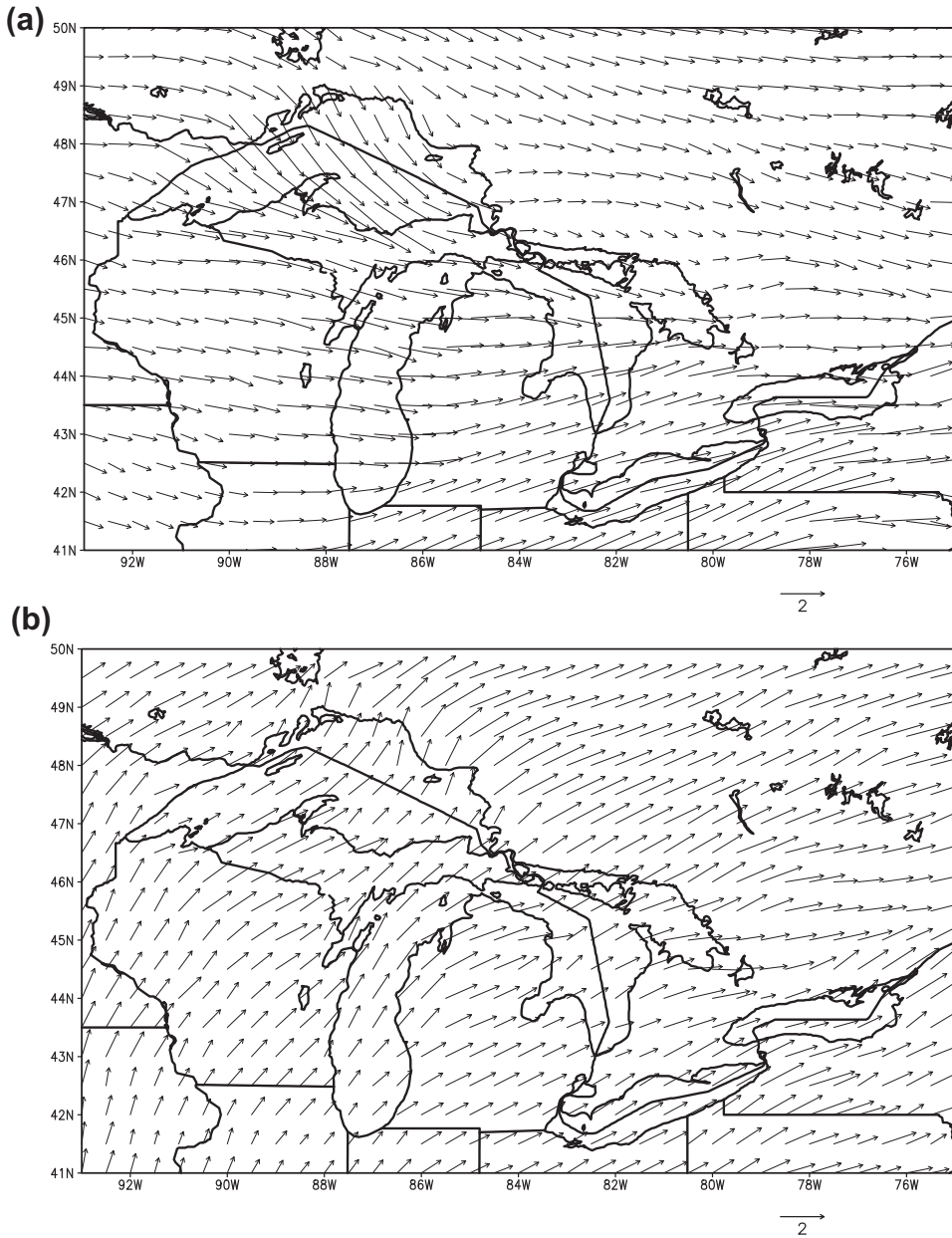


Fig. 3. NARR 16 years (1993–2008) mean surface winds during (a) winter and (b) summer. Unit: m/s.

Up to now, the direct current observations are still too sparse to define a circulation pattern in Lake Superior during winter because of severe weather conditions. The direct current observations at four moorings in the western part of the lake from mid-October 1966 through mid-May 1967 indicated that the currents generally paralleled the bathymetry, and one of the stations tended to indicate a prevailing counterclockwise pattern of general circulation. Driven by westerly winds with curl, both physical and numerical models predicted a cyclonic circulation in Lake Superior with variable depth (Lien and Hoops, 1978). Bennington et al. (2010) recent simulation shows a largely cyclonic circulation during winter. However, Pickett (1980) model predicted that, with west-southwest winds forcing, winter circulation in Lake Superior consists of two gyres: counter-clockwise in the west and clockwise in the east.

4.1.2. Lake Michigan

The modeled winter mean circulation in Lake Michigan (Fig. 6(a)) is cyclonic except for narrow areas in the northernmost

parts of the lake where an anti-cyclonic gyre persists. Two large cyclonic gyres are located in the north and south Chippewa Basin. In the middle of the lake, currents flow southward along the east and west channels on both sides of the mid-lake Plateau. The currents are weaker over the Plateau than those in the channels. The currents along the east coast are stronger than the currents along the west coast. The whole pattern is consistent with the direct winter current measurements during December 1962–September 1964 and June 1982–July 1983 (Gottlieb et al., 1989; Beletsky et al., 1999b) (Fig. 6(b)). Previous models (Allender and Saylor, 1979; Beletsky and Schwab, 2001, 2008) all produced a remarkably large-scale cyclonic circulation during winter.

4.1.3. Lake Huron

The modeled winter mean currents (Fig. 7(a)) in Lake Huron show strong southward currents along the west coast and the Alpena-Amberley Ridge (see Fig. 1), and northward currents along the east coast. The strong southward currents along the west coast

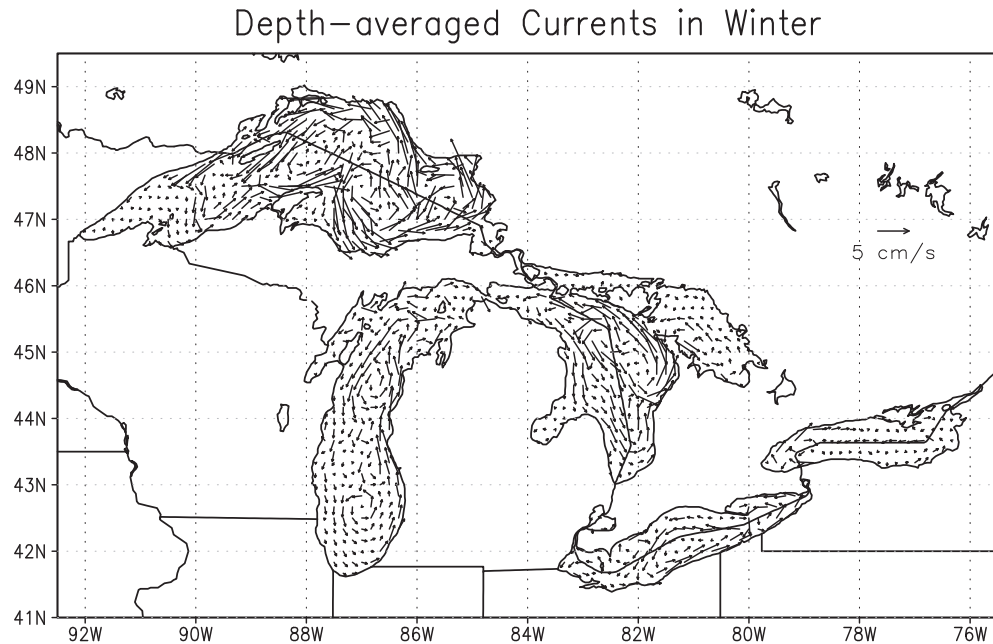


Fig. 4. Model depth-averaged winter currents in the Great Lakes from 1994 to 2008. Unit: cm/s.

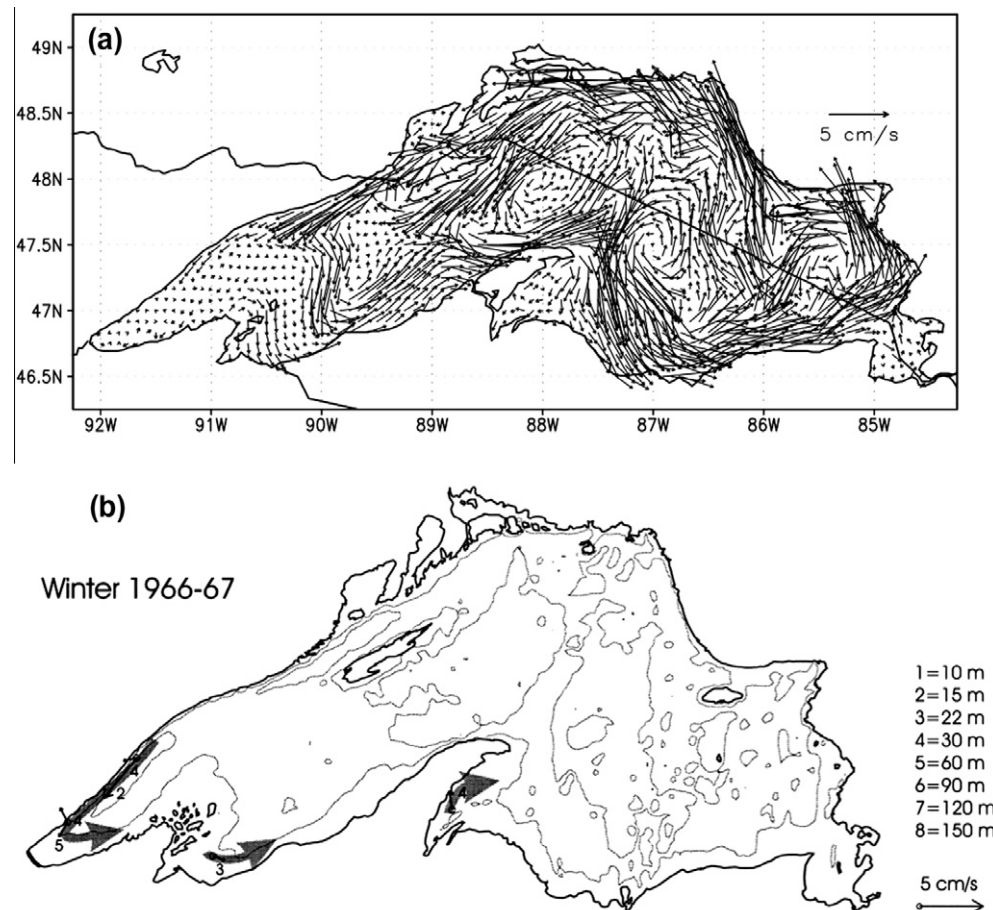


Fig. 5. (a) Modeled long-term mean winter circulation, and (b) Observed mean circulation during winter 1966–1967 (from Beletsky et al., 1999b) in Lake Superior.

were observed during winter 1974–1975 (Saylor and Miller 1976, 1979; Beletsky et al., 1999b) (Fig. 7(b)). However, the strong currents over the Alpena-Amberley Ridge can't be validated because

of insufficient observations. Nearly southward currents occupy most of the lake except a narrow band along the east shore. Georgian Bay also has a cyclonic circulation with a narrow band of

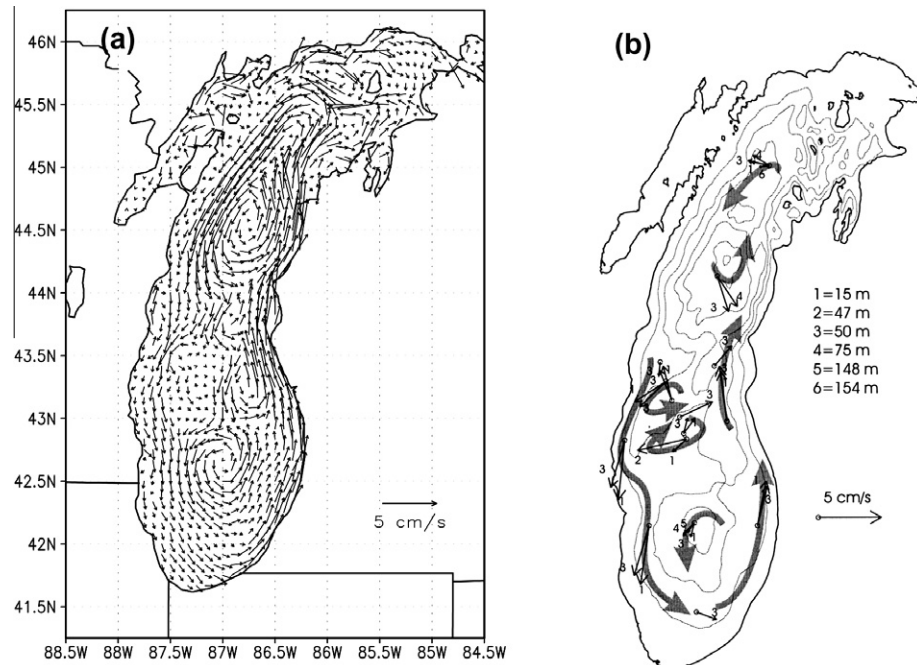


Fig. 6. (a) Modeled long-term mean winter circulation, and (b) Observed mean circulation during winter 1982–1983 (from Beletsky et al., 1999b) in Lake Michigan.

southward currents along the west coast, and northward currents occupying the other portions. The currents in Saginaw Bay are very weak. This typical pattern appears in November and persists until the following April. Recent model results show a similar circulation pattern (Sheng and Rao, 2006).

4.1.4. Lake Ontario

The model's depth-averaged currents in Lake Ontario (Fig. 8(a)) show a two-gyre pattern with an anticyclonic gyre in the west and a cyclonic gyre in the east. There are eastward currents along the north shore, westward currents along the long axis of the lake, and westward (eastward) currents along the west (east) portion of the south shore. The observed mean circulation during winter 1972–1973 (November–April) shows a two-gyre circulation with an anticyclonic gyre in the north and a cyclonic gyre in the south (Beletsky et al., 1999b) (Fig. 8(b)). Strong eastward currents were observed along the whole south shore, while the model produced westward currents along the west portion of the south shore.

Current data collected during the International Field Year for the Great Lakes (IFYGL) (April 1972–March 1973) suggest that the monthly winter currents in Lake Ontario consist of either one cyclonic (November, February, and March) or two counter-rotating gyres (May, December, and January) (Pickett, 1977). The observations during winter 1982–1983 show a one-gyre pattern in Lake Ontario (Simons et al., 1985). It seems that the winter circulation pattern in Lake Ontario has obvious interannual variability. The dominant pattern, according to Pickett and Rao (1976) comparison of the previous models, depends on the relative strength of the bathymetric-wind curl effects.

4.1.5. Lake Erie

The model currents show two-gyre circulations in both the central and eastern basins, which is consistent with the observations (Fig. 9(a) and (b)). Clockwise circulation occurs in the northern half of the lake and counterclockwise circulation in the southern half. Coastal flows are parallel to the shores, with westward return flow down the middle of the lake. The model currents also show a cyclonic gyre in the western basin of Lake Erie.

The observed currents from May 1979 through June 1980 show that Lake Erie had a typical two-gyre circulation pattern in the central lake during the winter months (Saylor and Miller 1983, 1987; Beletsky et al., 1999b) (Fig. 9(b)). In the eastern basin, although no observations are available near the north coast, the westward flow in the middle and eastward flow along the south coast implies that a two-gyre type circulation exists in the eastern basin (Fig. 9(b)). There are no direct current measurements in the shallow western basin.

4.2. Summer stratified period

In spring and summer, the heat flux on a lake surface causes density gradients that can produce currents comparable to wind-driven currents, and that makes lake hydrodynamics even more complicated. The final circulation pattern is the results of the combined effects of density driven, wind stress curl, topographic effect and the barotropic two-gyre response of a closed lake to the mean wind. Density driven circulation tends towards a one-gyre cyclonic circulation. The condition of no heat flux through the bottom boundary causes a dome-shaped thermocline, which is deeper near the shore and shallower in the deeper regions. A cyclonic circulation is built up to maintain geostrophic balance with the pressure gradient field (Schwab et al. 1995).

Fig. 10 shows model depth-averaged currents averaged over 1994–2008 during summer. There is a large cyclonic circulation in Lakes Superior, Huron, and Ontario. Lake Erie has a typical two-gyre pattern in the central basin and a cyclonic gyre in the eastern basin. Lake Michigan has a large cyclonic circulation in the north and an anti-cyclonic one in the south basin.

4.2.1. Lake Superior

The modeled upper 20 m mean currents in summer (Fig. 11(a)) show a large general counterclockwise circulation along the shores. The surface summer currents also show some gyres, such as cyclonic gyres to the southeast of Isle Royale occupying the Royale Basin, and around the east end of the lake; an anticyclonic gyre in the southwestern most region. These smaller gyres reflect in

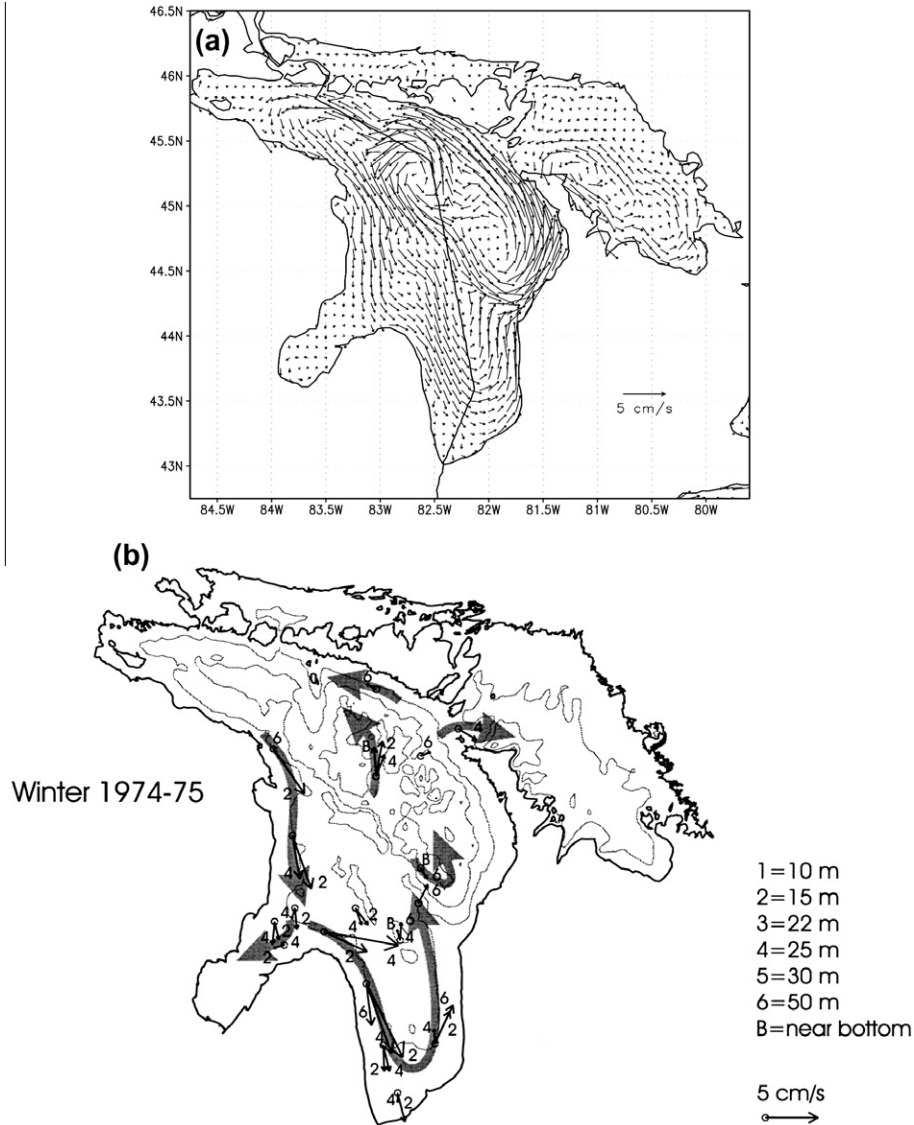


Fig. 7. (a) Modeled long-term mean winter circulation, and (b) Observed mean circulation during winter 1974–1975 (from Beletsky et al., 1999b) in Lake Huron.

some way the bottom topography. The coastal currents are very strong due to the effects of significant near-to-offshore temperature gradients and sloping topography as well. One special feature of Lake Superior is the Keweenaw current, which is often the strongest current in Lake Superior, located just off the north shore of the Keweenaw Peninsula. Zhu et al. (2001) pointed out that the topographic effect on the baroclinic gradient is the key mechanism of this current.

The whole pattern is generally consistent with the observations in 1967 and 1973 (Sloss and Saylor, 1976; Beletsky et al., 1999b) with some exceptions (Fig. 11(b)). For example, in the far west end of the lake, the currents observed near the north shore of Duluth Basin (see Fig. 1) were strong and flow westward along the shore during summer 1973 (Sloss and Saylor, 1976), and the currents near the south shore flow eastward during summer 1967 (Fig. 11(b)). The observations imply a cyclonic gyre in the far west end of the lake, while our model shows an anti-cyclonic gyre. Similar results were also found in Bennington et al. (2010) modeling forced by NARR.

4.2.2. Lake Michigan

For Lake Michigan, there are two big gyres, one is clockwise in the south, and the other is counterclockwise in the north

(Fig. 12(a)). The southern counterclockwise gyre was not seen in the mean summer circulation map by Beletsky et al. (1999b) (Fig. 12(b)), in which 1982–1983 current mooring data (Gottlieb et al., 1989) was used. However, in their report, Gottlieb et al. (1989) stated that the monthly-averaged currents are strongest during March and are very weak and slightly anticyclonic around the southern basin during June and July of both years (1982 and 1983). In their recent simulation, Beletsky et al. (2006) argued the existence of an anticyclonic gyre in the southern basin of Lake Michigan and stated that it was seen in all six years of their simulations (1998–2003), though the anticyclonic gyre in their results varies in size, shape and strength, and is smaller than our results. During the stratified period, density-driven and wind stress curl are the two major factors affecting lake circulation patterns (Schwab and Beletsky, 2003). The modeled anticyclonic gyre is most likely a product of the anticyclonic vorticity in the wind stress field.

There were four extensive surveys conducted during summer 1955 (June 28, June 29, August 9, and August 10), and the current pattern obtained by the dynamic height method indicated that a large anti-cyclonic eddy and three smaller ones existed in the lower parts of the southern basin (Fig. 12(c)). The existence of clock-

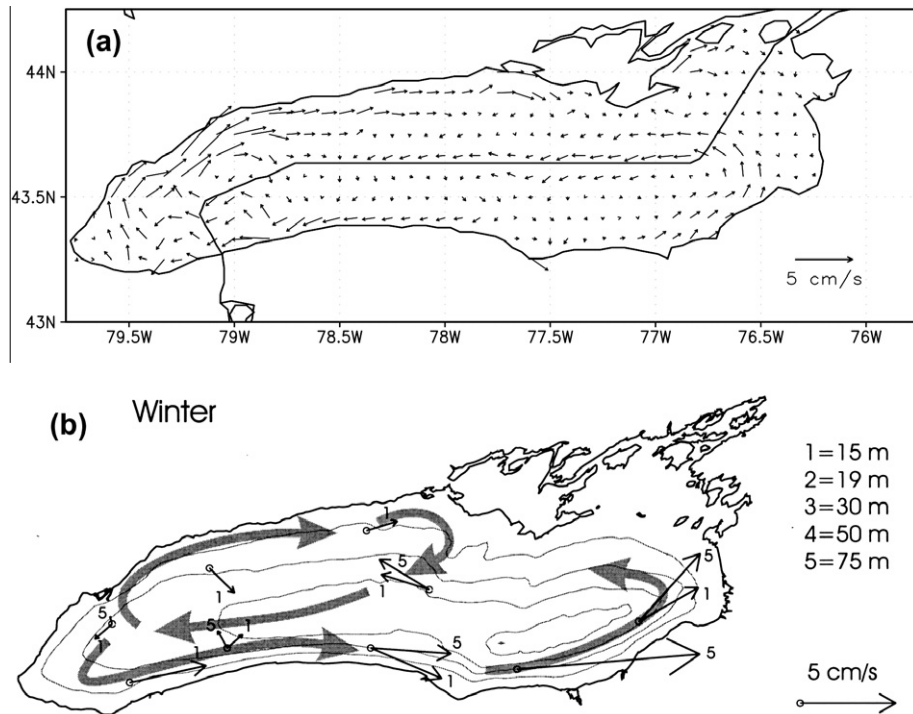


Fig. 8. (a) Modeled long-term mean winter circulation, and (b) Observed mean circulation during winter 1972–1973 (from Beletsky et al., 1999b) in Lake Ontario.

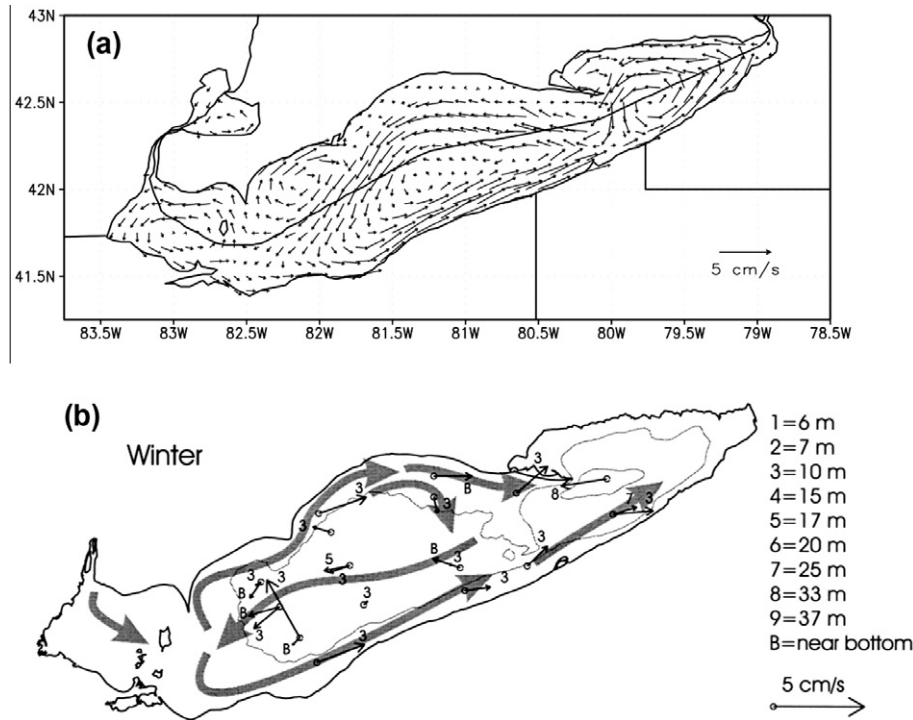


Fig. 9. (a) Modeled long-term mean winter circulation, and (b) Observed mean circulation during winter 1979–1980 (from Beletsky et al., 1999b) in Lake Erie.

wise eddies was substantiated by the distribution of water temperature, tracer materials, drifters, and the vertical sections of water temperature across the southern basin (Ayers et al., 1958).

4.2.3. Lake Huron

The model's top 20 m average currents during summer (Fig. 13(a)) shows a large cyclonic gyre in the upper and central portion of the lake, with a narrow current along the east shore

flowing northward, and southeastward currents occupying the rest of the upper and central portions of Lake Huron. There is a flow into Georgian Bay from Lake Huron. There are several smaller eddies in the central lake. In the lower portion of the lake, the mean circulation consists of three gyres: a clockwise gyre near the mouth of Saginaw Bay, an anticlockwise gyre off the southern east coast, and a clockwise gyre occupying the south end of the lake.

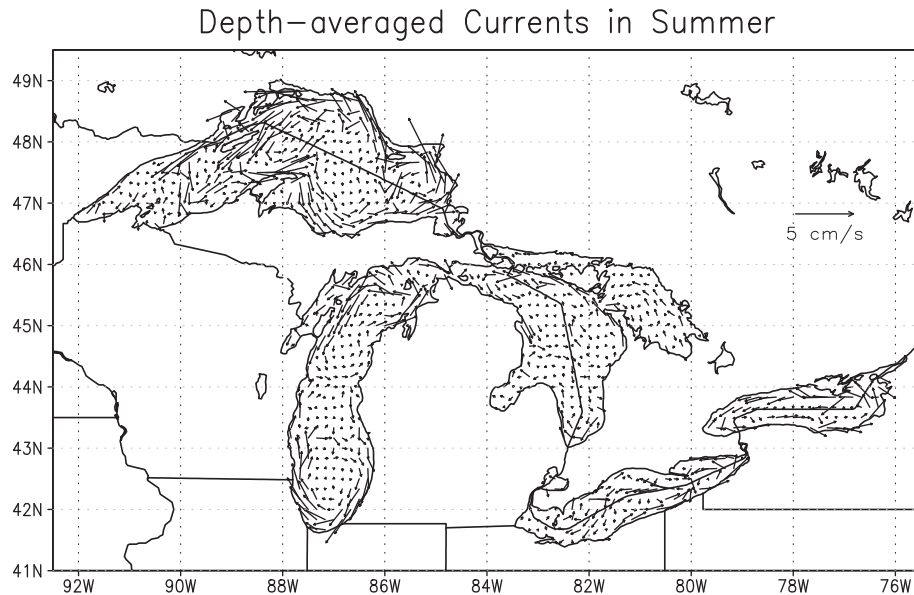


Fig. 10. Model depth-averaged summer currents in the Great Lakes from 1994 to 2008. Unit: cm/s.

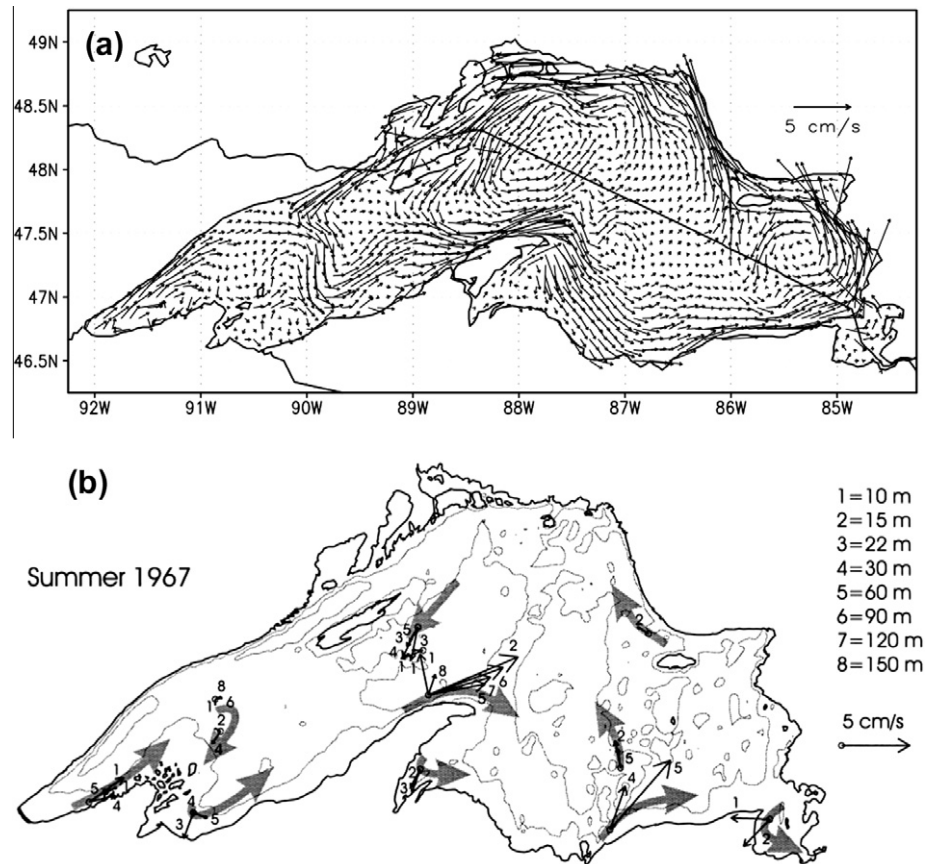


Fig. 11. (a) Modeled long-term summer mean top 20 m circulation, and (b) Observed mean circulation during summer 1967 (from Beletsky et al., 1999b) in Lake Superior.

Those features are quite similar to the circulation pattern observed in summer 1954 (Ayers et al., 1956) (Fig. 13(c)), which was constructed from the water density field by dynamic height methods. The constructed current patterns were more complex than Harrington's results, although the basic pattern in the upper and central portions of the lake appeared to be cyclonic (Harrington, 1895; Saylor and Miller, 1979). The current data collected during summer 1966 indicated that a cyclonic circulation dominates

the northern 2/3 of the lake at a 10-m depth, while the shallower southern portion has a more complex pattern (Sloss and Saylor 1975; Beletsky et al., 1999b) (Fig. 13(b)).

4.2.4. Lake Ontario

The model summer circulation in Lake Ontario shows a single cyclonic circulation with strong coastal jets along the north and south shores (Fig. 14(a)). The flow generally follows the contours

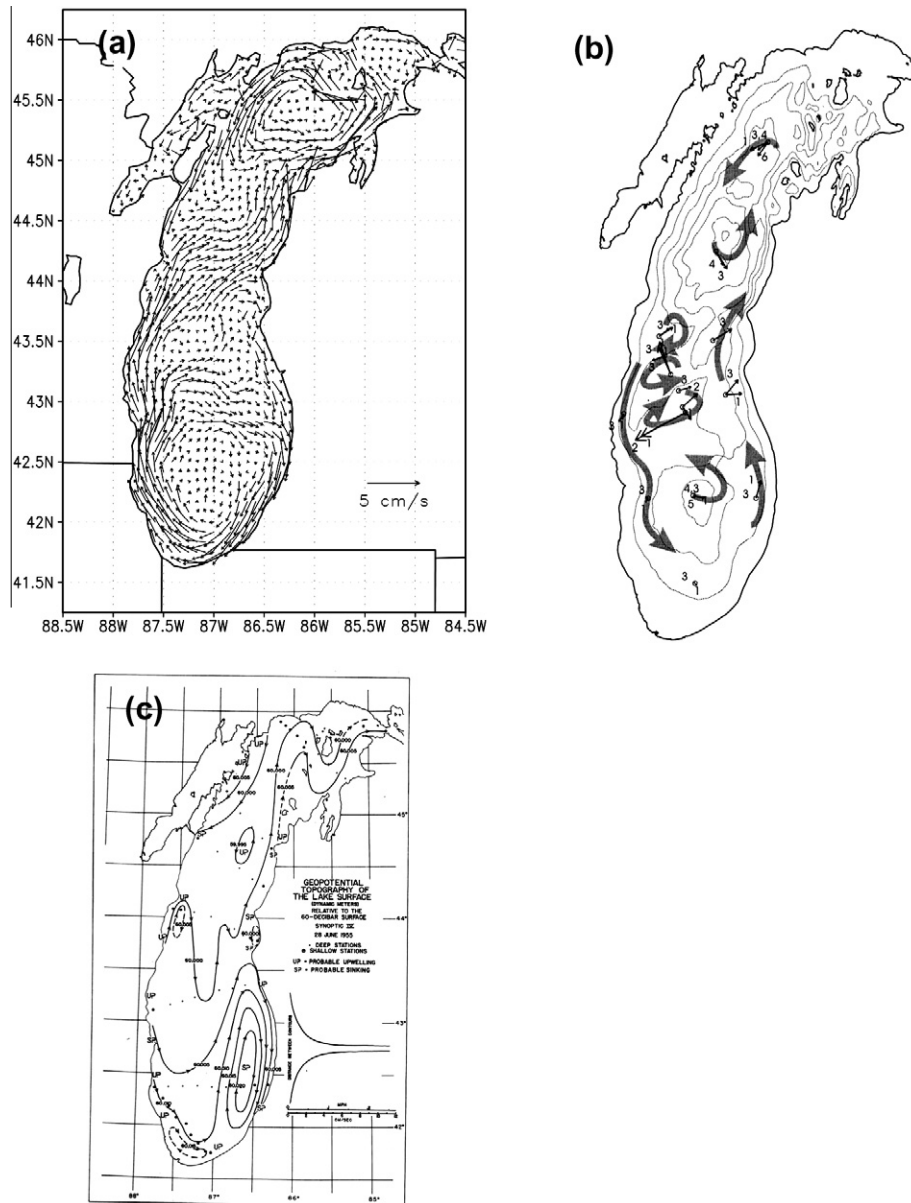


Fig. 12. (a) Modeled long-term summer mean top 20 m circulation, (b) Observed mean circulation during summer 1982–1983 (from Beletsky et al., 1999b), and (c) Surface current chart in June 28, 1955 (Ayers et al., 1958) in Lake Michigan.

of water depth around the lake's two deep basins. Monthly mean currents in June show a weak anti-cyclonic gyre in the northwestern portion of the lake. In July, the upper 20 m mean circulation shows a two-gyre pattern with an anti-cyclonic gyre in the west and a cyclonic in the east. Monthly mean currents in August and September show a single cyclonic circulation (not shown). It appears that the final circulation pattern depends mostly on the relative strengths of the thermally-affected mechanism and the wind-driven mechanism (Huang and Sloss, 1981). The cyclonic circulation in the central lake is very stable, while the anti-cyclonic gyre in the northwestern part of the lake is unstable.

Both surface and subsurface temperature and current data from earlier studies (Harrington, 1895; Rodgers and Anderson, 1963; Casey et al., 1966) suggest a single mean cyclonic circulation in Lake Ontario during its stratified period. During the intensive IFYGL investigation, current data from June to October 1972 suggests that the lake's resultant circulation consists of a dominant cyclonic gyre together with a small anti-cyclonic gyre in the northwest portion of the lake (Pickett and Bermick, 1977; Saylor et al., 1981; Beletsky

et al., 1999b) (Fig. 14(b)). Pickett and Bermick (1977) attributed that pattern to the results of the combination effects of one-gyre mechanism (density driven, variation in winds) and the barotropic two-gyre response of a closed lake to the mean wind. The mean wind may tend to generate two counter-rotating gyres, while variations in the wind and possibly thermal mechanisms tend to generate one counterclockwise gyre. The net result would be two counter-rotating gyres with a diminished clockwise cell and an enlarged counterclockwise cell. The relative size of these two gyres would vary with the relative strength of the one- and two-gyre mechanisms. Huang and Sloss (1981) carried out simulations for July 1972, and the model obtained a typical two-gyre pattern under constant atmospheric forcing, while a single cyclonic circulation was obtained under the time-dependent variable forcing. Huang et al. (2010) simulated summer circulation in 2006 and obtained a small and weak anti-cyclonic gyre in the western end of the lake using POM and ELCOM (Estuary, Lake, and Coastal Ocean Model), in addition to the large cyclonic circulation occupying a large portion of the lake.

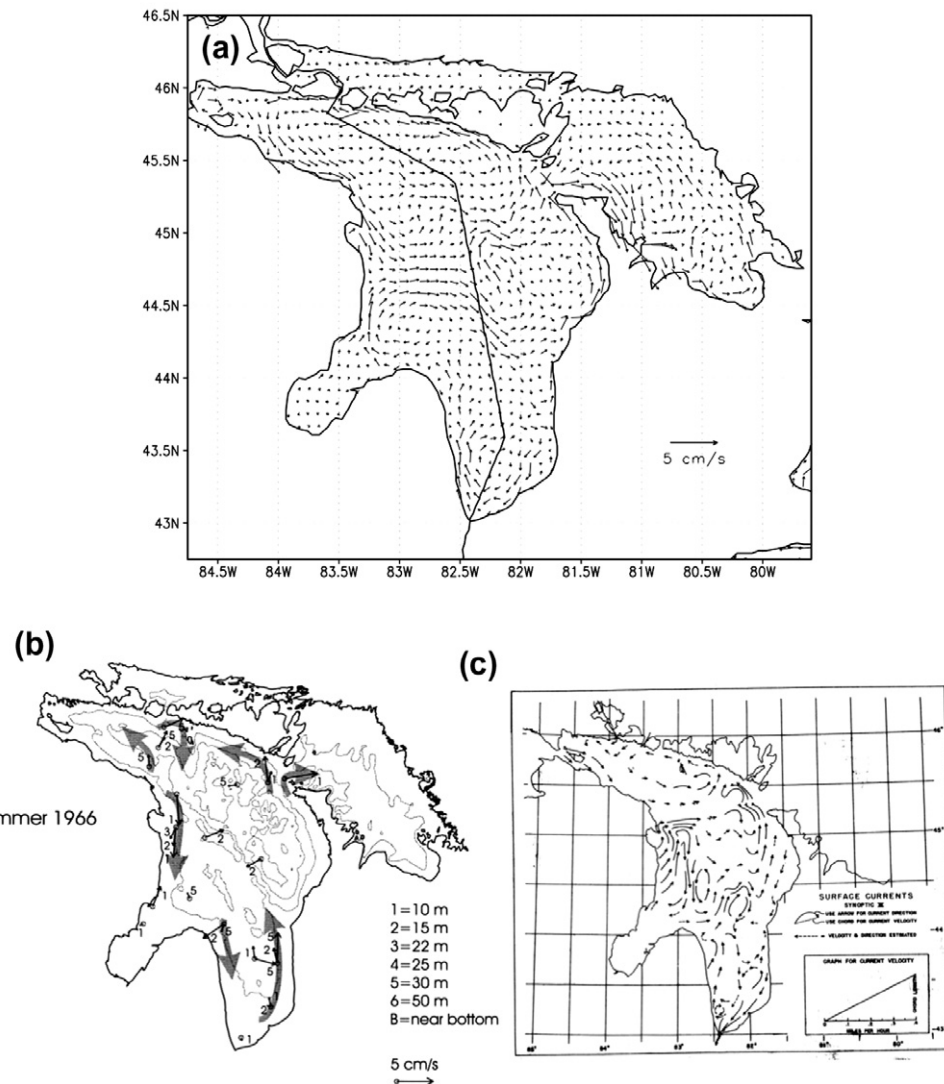


Fig. 13. (a) Modeled long-term summer mean top 20 m circulation, and (b) Observed mean circulation during summer 1966 (from Beletsky et al., 1999b), and (c) Surface current chart in August 25, 1954 (Ayers et al., 1956) in Lake Huron.

4.2.5. Lake Erie

Lake Erie has three dynamic quasi-isolated basins: western, central, and eastern. In the western basin, the model currents show an obvious northward flow along the Michigan shore, a southeasterly flow in the central, and a northeasterly flow in the eastern portion of the western basin (Fig. 15(a)). This pattern is consistent with that inferred from drifter cards (Hamblin 1971; Mortimer, 1987). Note that the lack of Detroit River inflow in the west end of the lake in the model may lead to artificial results in some degree.

There is a cyclonic gyre in the deepest eastern basin, which is consistent with the observations: Saylor and Miller (1987) reported that in the eastern basin, the observed monthly-averaged currents were cyclonic from May to August in 1979. A cyclonic flow during the summer in the eastern basin was also suggested by Hamblin (1971) because of a shallower thermocline in the basin's center and geostrophy. The cyclonic gyre seems to be a stable one because of its bowl-shaped bathymetry with deep water in the middle and shallow water on both sides.

In the central basin, the model summer mean currents show a typical two-gyre pattern: eastward flow along the north and south shores, southwestward flow along the middle axis, and a clockwise (counterclockwise) circulation gyre in the north (south) part of the

central basin. The pattern is different from that observed during summer 1979, when the observed current data indicated an anti-cyclonic circulation dominating the central basin in August and September (Saylor and Miller, 1987; Beletsky et al., 1999b) (Fig. 15(b)). However, the pattern is quite similar to those simulated for summer 1994 by León et al. (2005) and Schwab et al. (2009). The anti-cyclonic circulation during summer 1979 was probably caused by wind curl. Recently, the observations in central basin of Lake Erie reveal a persistent basin-wide bowl-shaped thermocline accompanied by anticyclonic circulation in August and September 2005 and August 2007. It is suggested that the unusual bowl-shaped thermocline is the result of Ekman pumping driven by anticyclonic vorticity in surface winds (Beletsky et al., 2012).

5. Temperature

5.1. Surface water temperature

Figs. 16 and 17 show the observed and modeled long-term monthly mean lake surface temperatures (LST) in February, May, August, and November, respectively, to demonstrate the annual evolution of the LST in the Great Lakes.

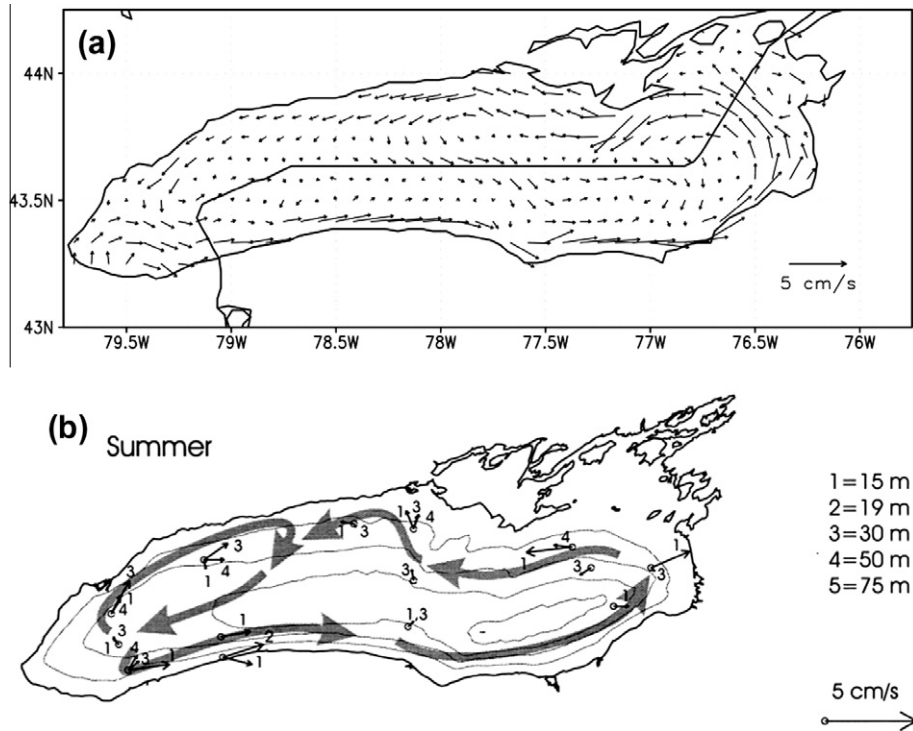


Fig. 14. (a) Modeled long-term summer mean top 20 m circulation, and (b) Observed mean circulation during summer 1972–1973 (from Beletsky et al., 1999b) in Lake Ontario.

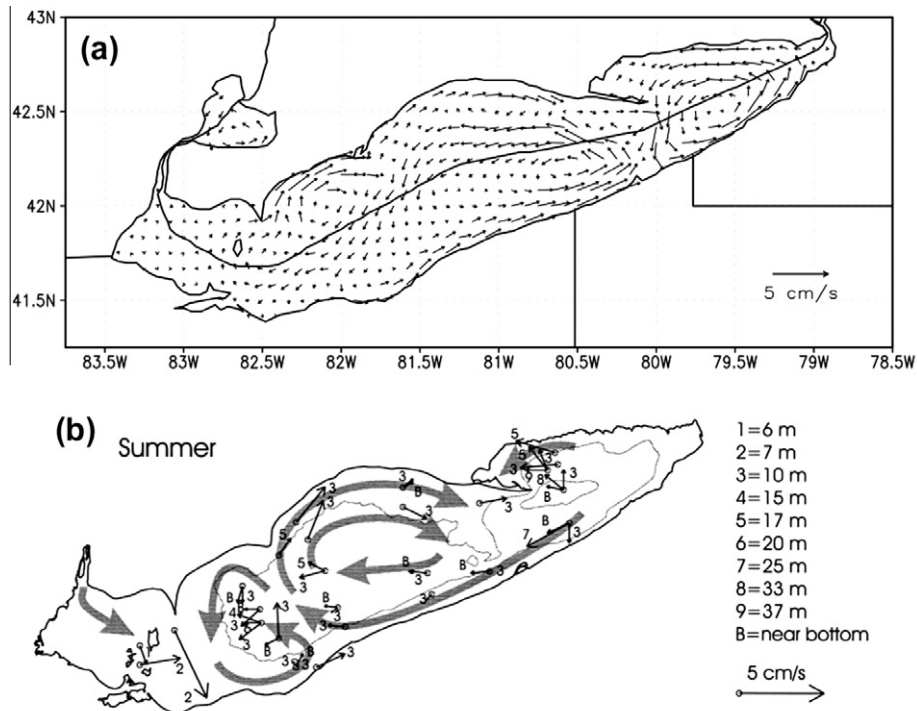


Fig. 15. (a) Modeled long-term summer mean top 20 m circulation, and (b) Observed mean circulation during summer 1979–1980 (from Beletsky et al., 1999b) in Lake Erie.

In the middle and late winter, between January and early March, the water is colder than the temperature of maximum density (4°C) everywhere. Both the model and observations show that the water temperatures ($\sim 2\text{--}3^{\circ}\text{C}$) in the deep basins are higher than those in the near shore areas ($\sim 1^{\circ}\text{C}$), because the shallower water is more easily cooled. Lakes Michigan and Ontario are warmer than the other

lakes. The shallowest lake, Lake Erie, has the lowest surface temperature. This winter condition usually lasts until spring.

Mean surface temperature in May features cold central lake water surrounded by warm near shore waters. This is because the shallow near shore waters are heated more quickly than the deep basin waters during spring warming.

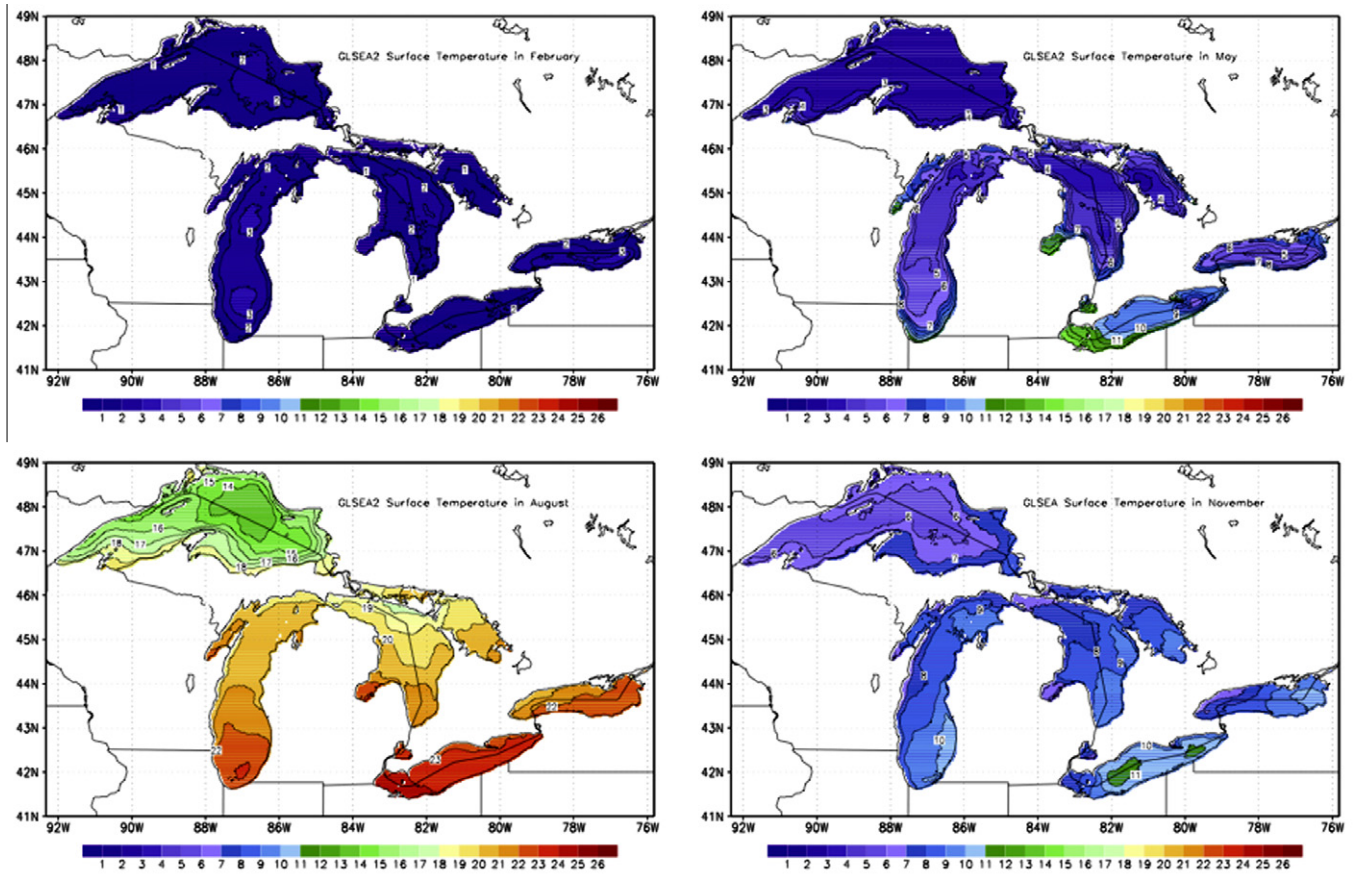


Fig. 16. GLSEA monthly climatology of lake surface temperature for the period 1995–2008 in February, May, August, and November.

As the surface heating progresses in early spring, the surface reaches the temperature of maximum density, and the shallow areas generally become stratified before deeper areas. In large lakes this condition may persist for weeks, during which a temperature front known as a “thermal bar” forms between the stratified shallower water and the cold unstratified mid-lake water (Rodgers, 1966; Schertzer, 2003). The downwelling of dense water at the thermal bar acts as a barrier to horizontal mixing.

The thermal bar generally forms parallel to shore and moves toward the lake center as deeper areas of the lake gradually stratify. As shown in Fig. 18, thermal bars first appear in Lakes Erie and Michigan in early April. The thermal bars in Lake Erie start in the western basin and then propagate eastward. The thermal bar in Lake Michigan appears first in the southwest tip and then propagates northward along the east and west shores. For Lake Huron, the thermal bar first forms in the southern lake on April 10. On April 20, the thermal bar disappears in Lake Erie, but still exists and develops in Lakes Michigan, Huron, and Ontario. Ten days later, the thermal bar develops along the southern shore of Lake Superior and then moves northward. Due to the shape and position, the duration of the thermal bar varies lake by lake: it is the largest in Lake Michigan and smallest in Lake Ontario.

After July, the lakes are strongly stratified. In August, with intensified stratification, surface heating is almost confined above the thermocline; thus surface water in the deeper basins warms up. Temperature differences between the deep water and the shallow shore waters almost disappear, and south-north temperature gradients determined mainly by latitudes dominates the Great Lakes (Figs. 16 and 17).

During fall, the lakes start to cool down. Rapid cooling occurs from October to December. The cooling is from north to south

and from the coast to the deeper basin (Figs. 16 and 17). In November, the observations show that surface water temperature in western portions of Lakes Michigan, Huron, and Ontario is lower than that in the eastern portions, which are reproduced by the model to some degree. Regarding this pattern, the simulation is better in Lakes Huron and Ontario than in Lake Michigan. For Lake Erie, the model reproduces well the feature of cold shallow and warm basin waters.

5.2. Vertical thermal structure

To validate the model's vertical thermal structure, model and observed temperature profiles at station CM1 (see Fig. 1) for 1998 are presented in Fig. 19(a) and (b), respectively. Observations show a well-mixed water column during winter and spring (January–April) with water temperature around 4 °C, when the maximum density of fresh water occurs. The stratification starts in May. Surface heating continues to strengthen stratification, which was the strongest during August through September. The mixed-layer depth during summer 1998 was about 10–15 m at CM1. The thermocline was very sharp with temperature decreasing from 21 °C to 10 °C within 10 m. In early October, the surface mixed layer started deepening due to surface cooling and strong winds, and it was about 30 m at the end of October. The thermocline during October is the sharpest all year round, only about 5 m in vertical extent. During November and December, the stratification was almost destroyed due to strong surface mixing.

Compared with observations, the evolution of thermal structure at CM1 was basically reproduced by the model, though there are still some discrepancies (Fig. 19). Similar to the observations, from January to mid-April, the model water temperature at CM1 was

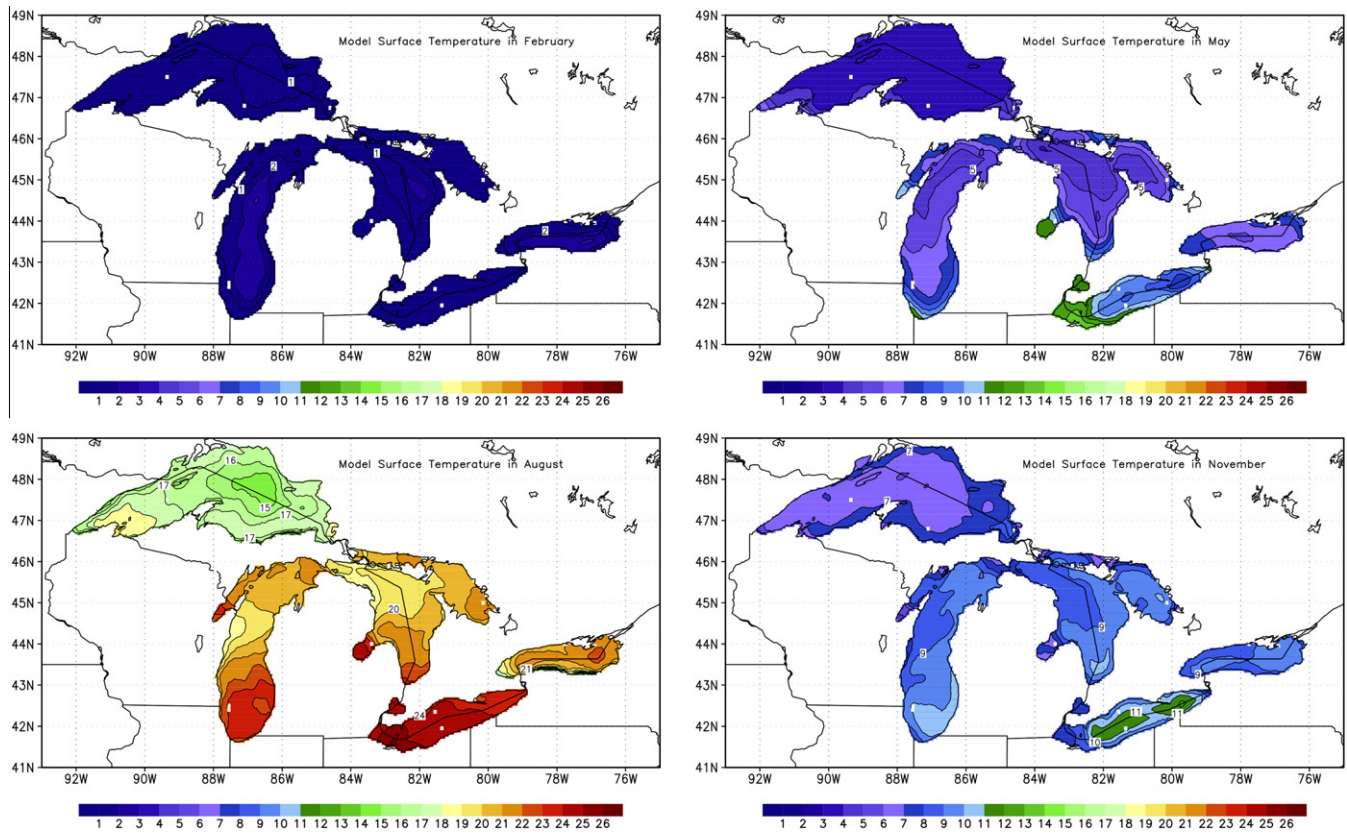


Fig. 17. Model monthly climatology of lake surface temperature for the period 1995–2008 in February, May, August, and November.

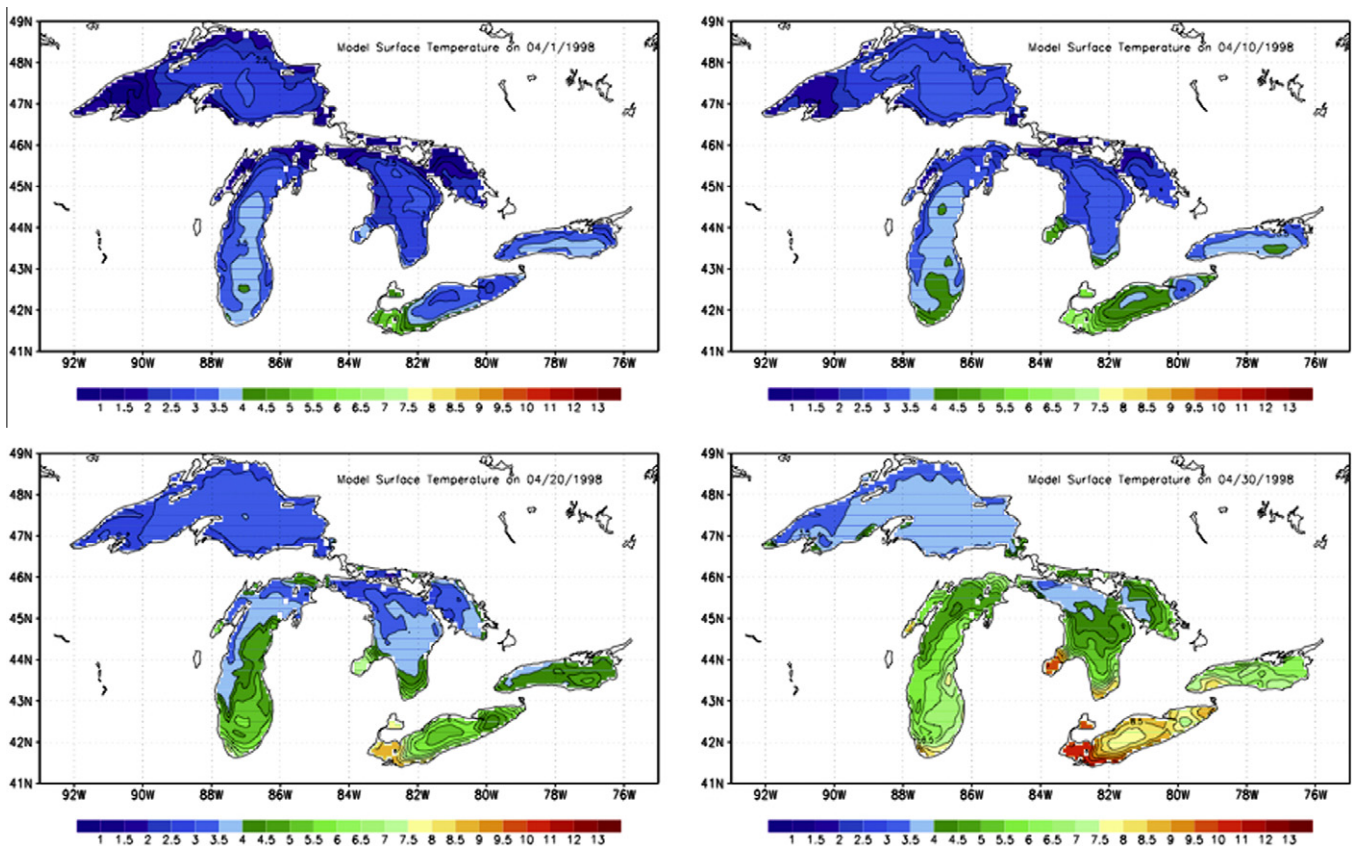


Fig. 18. Model daily surface temperatures during April 1998.

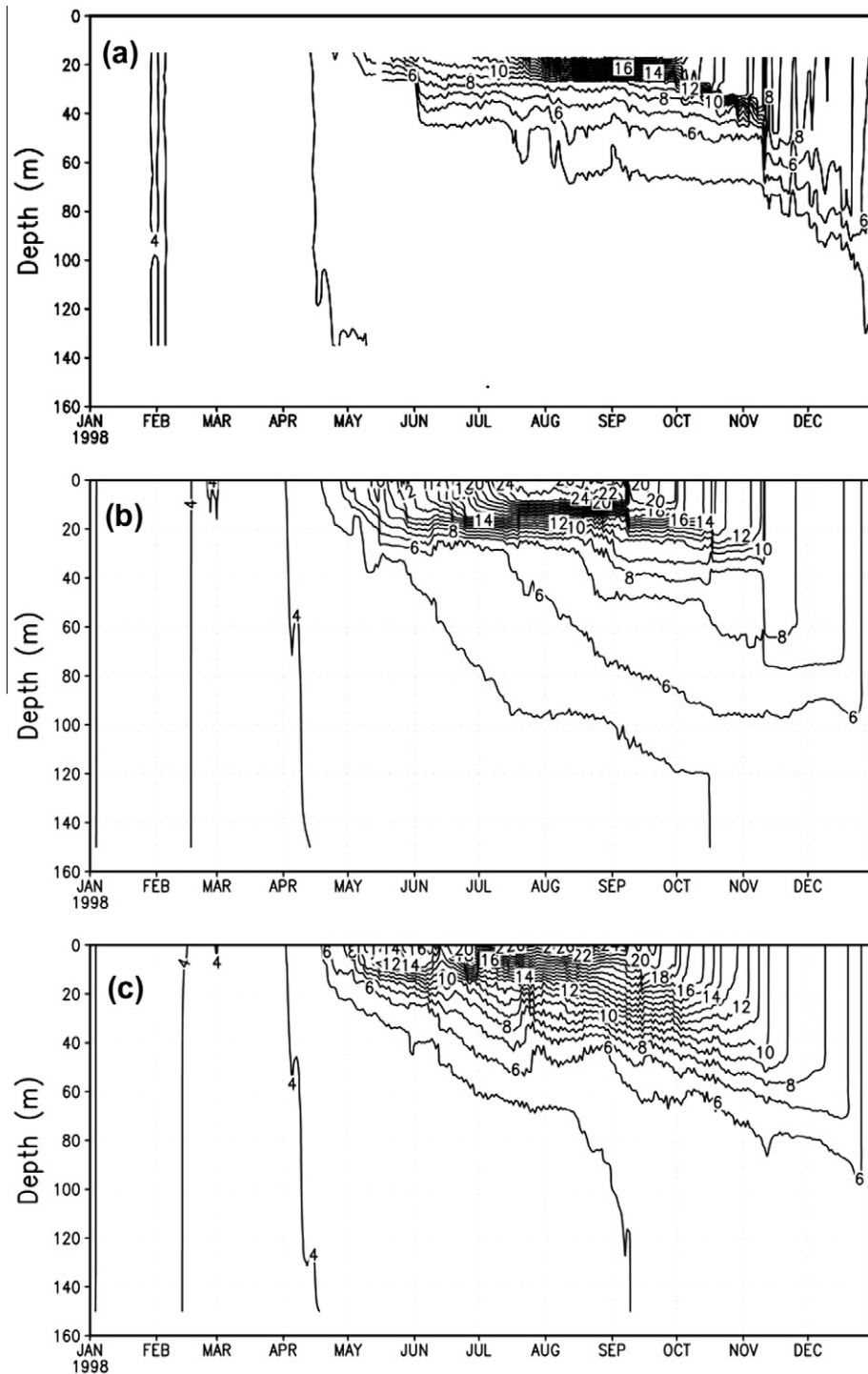


Fig. 19. Temperature profiles in CM1 during 1998: (a) Observation, (b) model with surface wind wave mixing, and (c) model without surface wind wave mixing.

around 4 °C, and the whole water column was completely mixed. The spring warming started around mid-late April, which is a little earlier than the observations (around early May). From late April to the end of June, water temperature continues to increase, and a weak stratification develops in the upper 30 m. Surface heating strengthens the stratification. In the model, an obvious thermocline was produced during mid-late June. The thermocline was located between 20–30 m. Surface heating strengthens the stratification from July through August. During August, when the

stratification was the strongest, the surface mixed layer depth was less than 10 m, and the thermocline was between 10–30 m, which is close to the observations. However, the water temperatures below the thermocline are higher than the observed temperatures during the summer, indicating that more heating was transferred to the deeper waters in the model. During autumn, strong mixing caused by cooling and strong winds deepens the mixed layer until late December, when a nearly isothermal condition exists throughout the whole water column. Strong winds

associated with the passage of a very strong storm in the Great Lakes region around November 10, 1998 accelerated the destruction of stratification, which was successfully simulated (Fig. 19(b)).

To assess the effects of the surface wind-wave mixing scheme, we conducted an experiment, in which the scheme was excluded. The temperature profile in the CM1 is shown in Fig. 19(c). Comparing the model results to the observations, it is found that without surface wind-wave mixing, the upper mixed layer is about 5 m, which is quite shallow, and the thermocline is too diffuse and weak, which is located between 5 and 40 m. Without a sharp thermocline, surface heating is transferred easily to the deeper portion of the water column, thus, at the depths beneath the thermocline, about 2 °C warmer water temperature can be observed in the no wave mixing modeling. While the model with the surface wind-wave mixing produces a more accurate mixed layer depth of 15 m in summer and a sharp thermocline, which is located between 20 and 30 m.

The modeled long-term monthly mean temperatures along transects in the five lakes are shown in Fig. 20 with an interval of 2 months to further reveal the main features and differences of cooling and warming processes in the lakes. In all the Great

Lakes, cooling starts in autumn when the summer surface mixed layer deepens because of stronger winds and buoyancy loss, and destroys the stratification. During October, the shallow central Lake Erie is well mixed from top to bottom with temperature around 16–17 °C. During November (not shown), most of the water column is well mixed along transects in the other deep lakes, with a weak stratification remaining in the bottom layers. The mixing is effective at depths as great as 60–70 m in Lakes Michigan, Huron, and Ontario, and even further to 160 m in Lake Superior in November. During December, all the Great Lakes have a well-mixed water column from top to bottom with a temperature around 5–6 °C, which is called the autumn overturn.

Below 4 °C, water becomes less dense as it cools. Further cooling in winter leads to inverse temperature stratification (cold surface layer water over the warm interior water), a layer of low density water colder than 4 °C, but warmer than 0 °C forms on the surface. The inverse temperature stratification normally begins after mid-December in the Great Lakes. In the model, Lake Superior has a significant inverse temperature stratification, which begins in early January and ends in April, when surface heating increases the surface temperature to near 4 °C. Lake Ontario also developed an

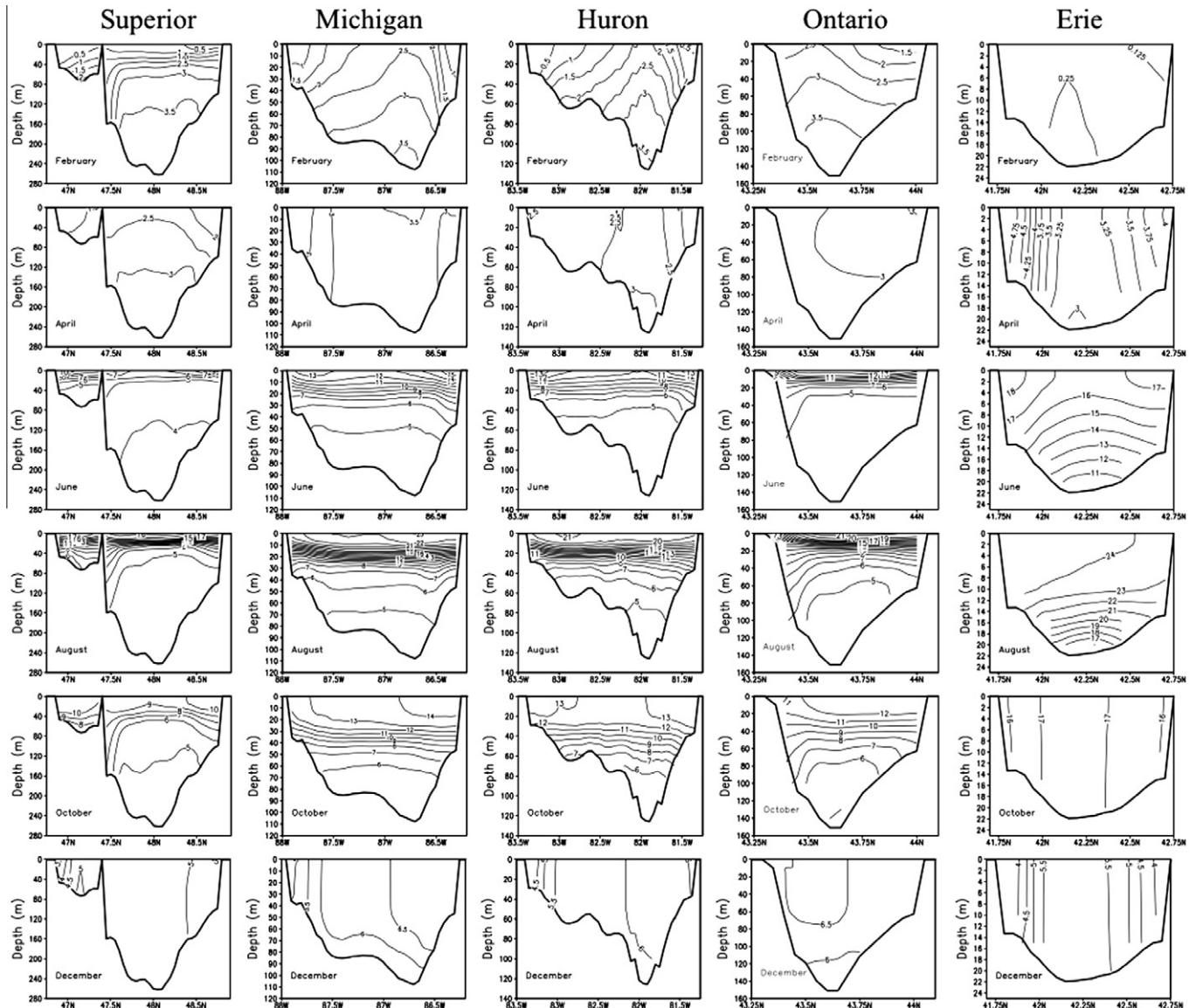


Fig. 20. Vertical sections of long-term monthly mean temperature (°C) along transects in five lakes.

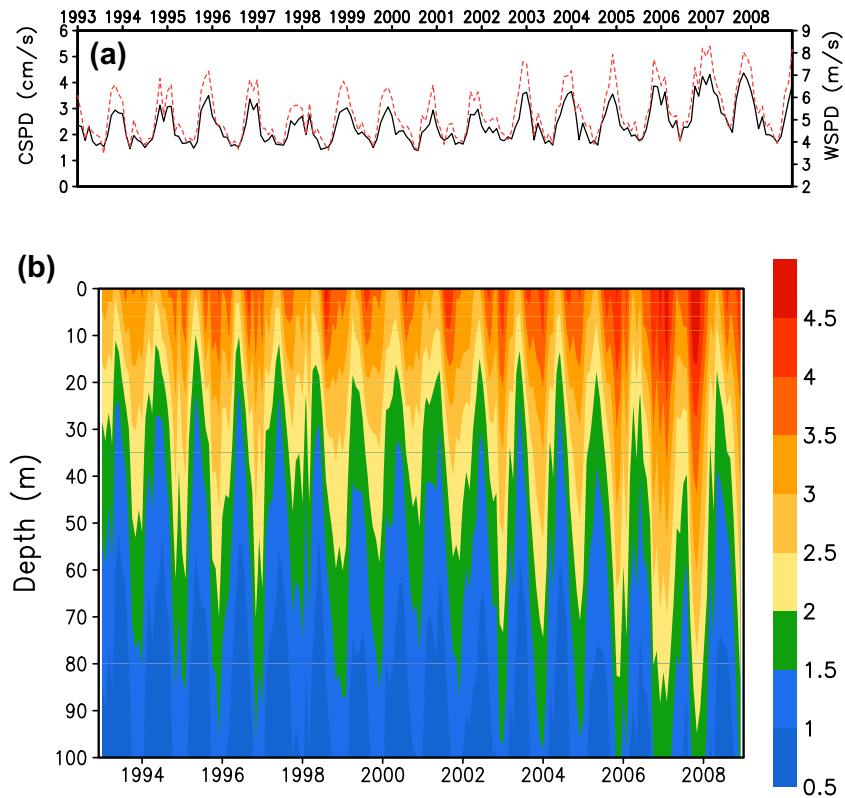


Fig. 21. (a) Modeled monthly mean domain averaged integrated current speed (black solid line, unit: cm/s) and wind speed (red dashed line, unit: m/s) from 1993 to 2008; (b) Time-vertical section of modeled monthly mean current speed from 1993 to 2008 (unit: cm/s).

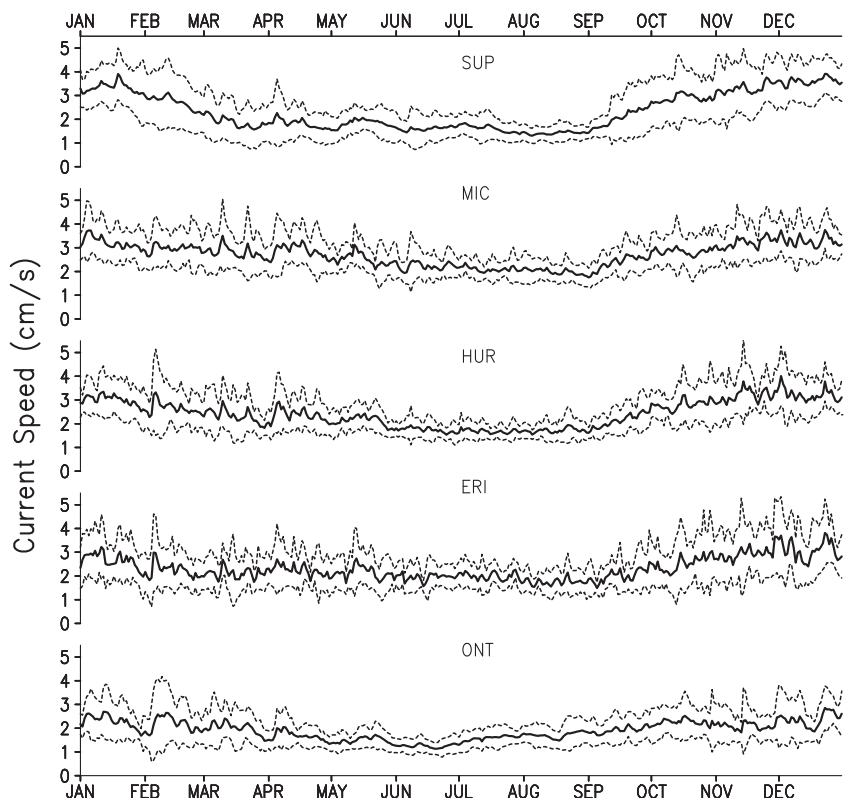


Fig. 22. Long-term (1994–2008) daily mean current speeds (solid) and standard deviations (dashed line) for each lake and the whole Great Lakes.

obvious inverse temperature stratification from February to March. In southern Michigan, along a transect from Milwaukee to Muskegon, an inverse temperature stratification develops in near shore water on both sides. In Lake Huron, a weak inverse temperature stratifications first develops on both near-shore sides and then develops in the central basin from January to February. Lake Erie has a very weak inverse temperature stratification during February.

During March, when warming starts, surface water temperature reaches around 4 °C, strong vertical mixing begins, the reverse stratification disappears, and the whole water column water is well mixed from top to bottom, which is called the spring overturn. This process is very important in that it allows relatively large amounts of oxygen to reach the bottom of the lake. Otherwise, oxygen would have to reach the bottom by the relatively slow process of diffusion. The spring overturn appears around late March in all lakes except Lake Superior where the well-mixed state occurs around mid-April.

Warming is faster in the near shore area than in the central basin. Near-shore water first reaches 4 °C, and the shallower near shore temperature increases rapidly with the development of the “thermal bar”. Then, a diffusive stratification forms at the surface after the lakes have been heated to a temperature fractionally above 4 °C. All the lakes develop stratification during May. After a thermocline has been produced, surface temperature rapidly increases until mid-July. After July, the lake is strongly stratified. A sharp vertical temperature gradient (thermocline) is present all across the lakes.

The above analysis shows that the model successfully reproduces the annual temperature cycle in the Great Lakes and some important thermal structure features, such as the well-mixed water column in early spring and late fall, inverse temperature stratification in winter, and strong stratification during the summer. The mixed-layer depth during the stratified period is also well simulated when the surface wind-wave mixing scheme is included.

6. Annual cycle and interannual variability

6.1. Current speed

The modeled monthly depth-averaged current speed for the whole Great Lakes exhibits obvious annual and interannual variations (Fig. 21(a)). The fluctuations in current speed generally follow the wind speed, and the correlation between them is 0.96. The years of 1994, 1997, and 2000 had the lowest annual mean current speeds (2.05, 2.07 and 2.08 cm/s, respectively), while the year of 2007 had the highest annual mean current speed (3.4 cm/s).

Fig. 21(b) shows the whole basin averaged vertical structure of current speed from 1993 to 2008. Most of the energy is confined within the upper 50 m with the highest current speed near the surface. During the winter, the energy penetrates much deeper than summer, because the stratification during the summer prevents energy from transferring into the lower layer. The high-speed tongue (>2 cm/s) extends from the surface to about 50 m during the winter and only about 15–20 m during the summer. The extension

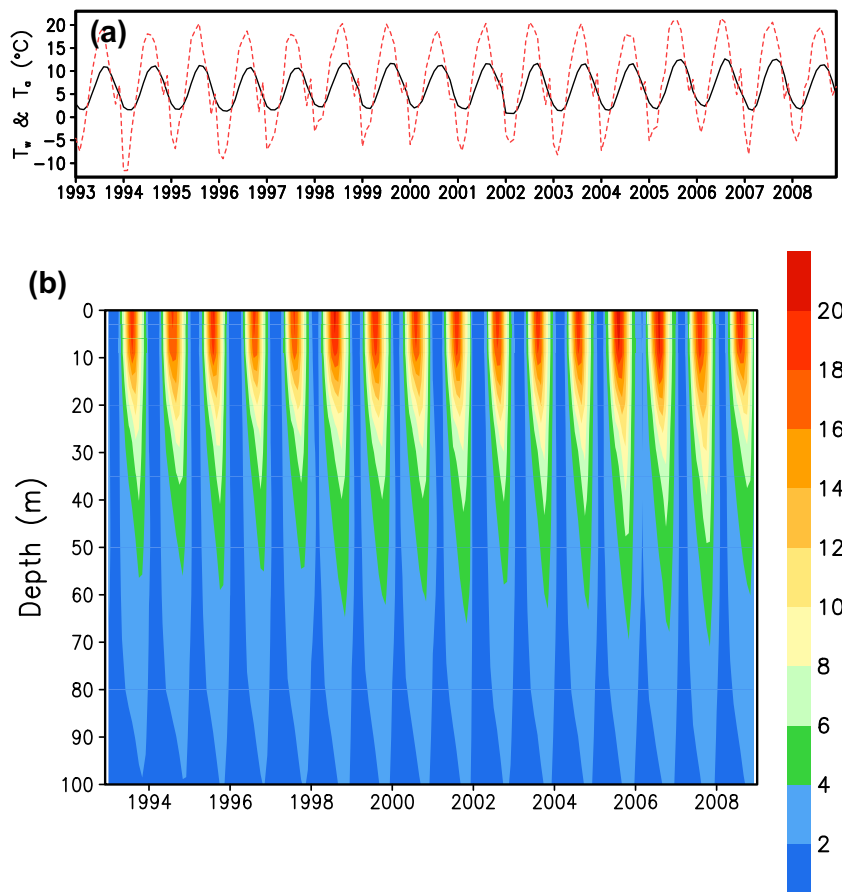


Fig. 23. (a) Modeled monthly mean domain averaged integrated water temperature (black solid line, unit: °C) and surface air temperature (red dashed line, unit: °C) from 1993 to 2008; (b) Time-vertical section of modeled monthly mean domain averaged water temperature from 1993 to 2008 (unit: °C).

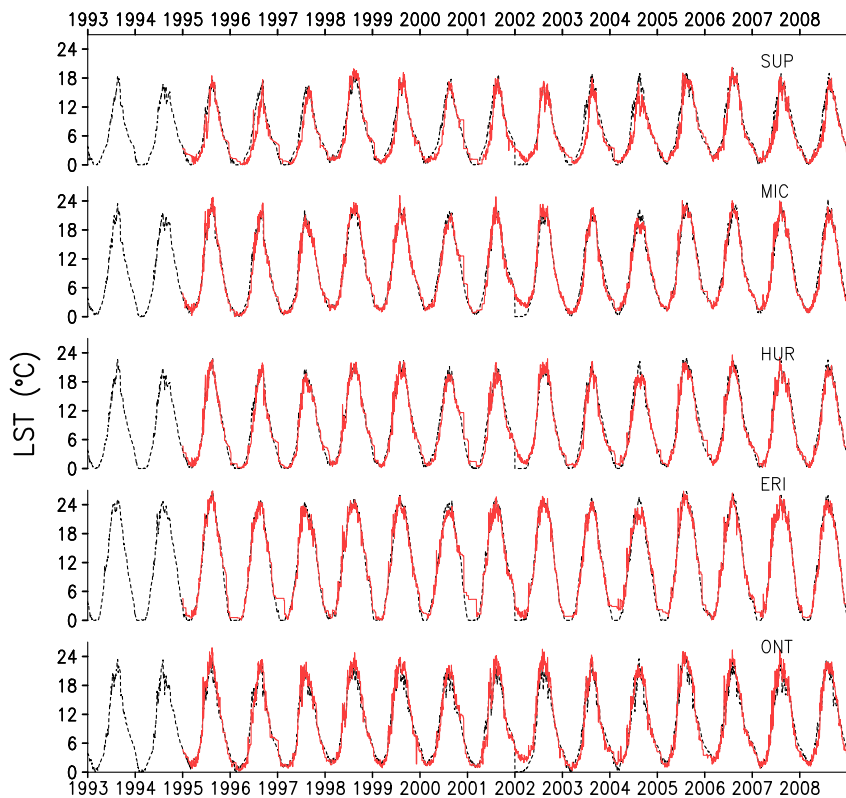


Fig. 24. Model (dashed line) and observed (solid line) daily mean lake wide averaged surface temperature for each lake from 1993 to 2008.

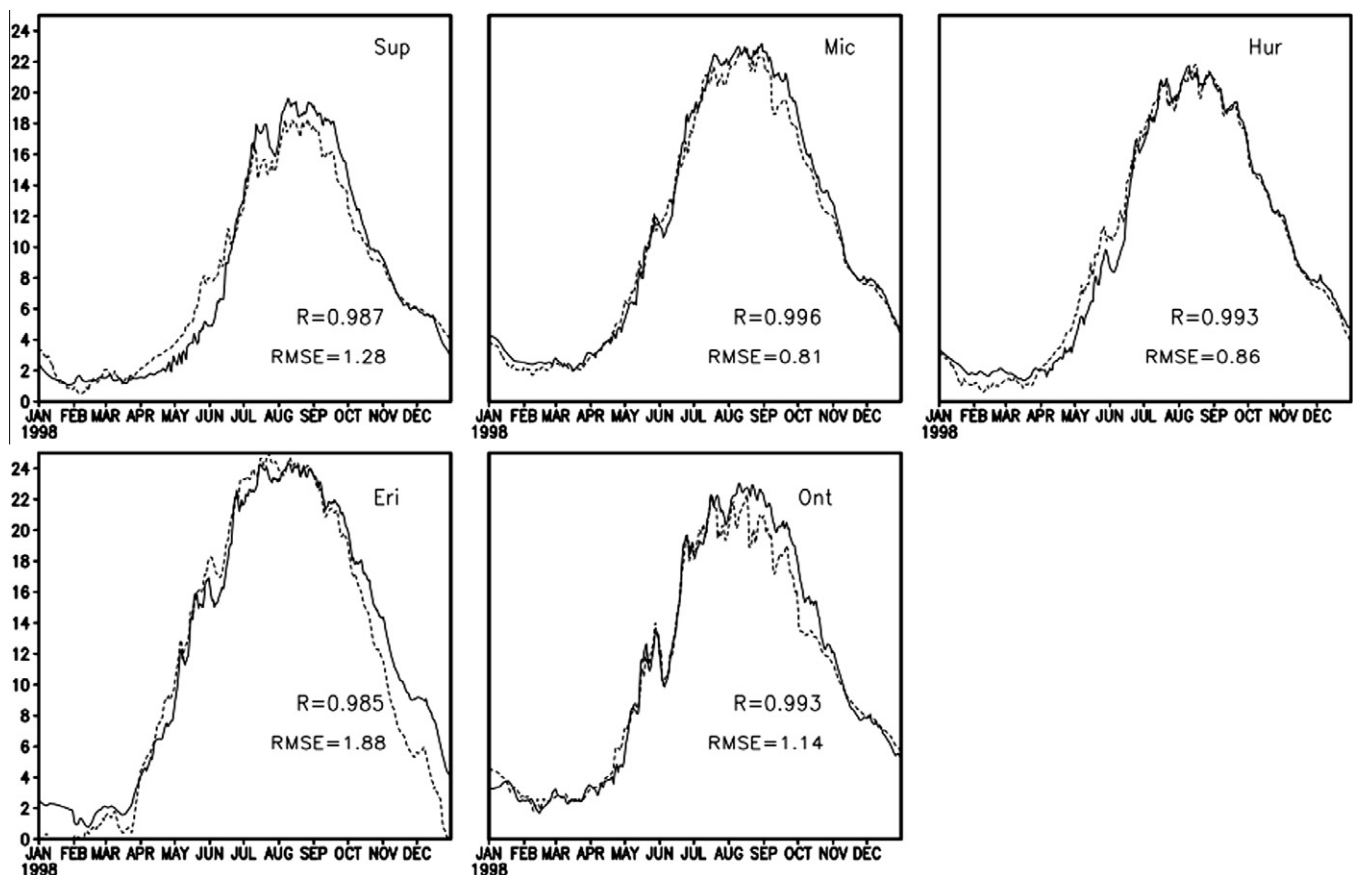


Fig. 25. Model (dashed line) and satellite observed (solid line) lake wide averaged surface temperature for each lake during 1998. Correlations and RMSE are also shown.

changes over years, for example, the high speed tongue extended to about 45–50 m during winter 2000/2001 while it was below 90 m during winter 2007/2008. The extension has a deepening trend during the modeling period, which is consistent with the upward trend in the wind speed.

Fig. 22 shows the daily climatology of depth-averaged current speed along with the standard deviation (STD), which indicates that current speed in the Great Lakes has a significant annual cycle with a large fluctuation. Lake wide mean current speeds peak in winter and decay over spring, reaching a minimum during late summer. As the model does not have an ice model during winter, the magnitude in winter may be exaggerated, and should be viewed with caution, although winter current speed is usually largest among all the seasons. Current speeds are relatively constant during summer. The winter mean current speed for the whole Great Lakes is 2.46 cm/s, while the summer mean current speed is 1.70 cm/s (**Table 1**). Lake Michigan has the strongest mean current both in winter and summer, while Lake Ontario has the weakest mean current (**Table 1**). Lake Superior has the largest STD both in winter and in summer. Lake Ontario has the smallest standard deviation during summer, and Lake Michigan has the smallest STD during winter. The STD is larger during winter than during summer for all five Great Lakes.

6.2. Temperature

Fig. 23(a) shows the integrated water temperature of the whole water column for the whole model domain from 1993 to 2008. The integrated temperature has an obvious annual cycle with the minimum in March and the maximum in September, which lags the surface air temperature by about a month. The simultaneous correlation between them is 0.86. The correlation reaches the maximum (0.94) when the surface air temperature leads the integrated water temperature by a month.

The whole basin averaged vertical structure of water temperature from 1993 to 2008 shows a similar annual cycle repeats over years (**Fig. 23(b)**). It is also clear that the onset and duration of the positive stratification, the vertical extension of the water with temperature greater than 4 °C (warm tongue) all changes over the years. For example, the winter 1997/1998 was a very mild winter due to a strong El Niño events (Bai et al., 2012), the onset and duration of the stratification was earlier and longer than normal, and the warm tongue could extend to 65 m during 1998. During 1997, the extension of the warm tongue was only about 55 m. The warm tongue extended to 70 m in 2007, which is the deepest during the modeling period.

The modeled daily lake averaged surface temperatures from 1995 to 2008 match well with the observations (**Fig. 24**). **Fig. 25** presents the model- and GLSEA-averaged LST during 1998, which shows that the model captures both the seasonal cycle and synoptic scale events successfully. All lakes had a minimum temperature around early March and a maximum in mid-August. The correlations between model results and observations for each lake are all greater than 0.98. Root mean square error (RMSE) varies lake by lake, ranging from 0.86–1.88 °C (**Table 2**). Synoptic scale warm-

ing and cooling events were both well captured. For example, the model captures two remarkable cooling events on 26–31 July and 15–18 August.

Fig. 26 indicates that the model accurately simulated the LST climatology and its variation in all five lakes. The modeled shapes of the seasonal cycle are consistent with observations. Both observed and modeled LST show larger variations during summer than during winter. From January to March, model LST in all five lakes is lower than the observations. From April to December, the simulated LST matches the observations well. As shown in **Table 3**, Lakes Superior and Huron have a small warm bias of 0.42 and 0.04 °C, respectively. Lakes Michigan, Erie, and Ontario have a small cold bias of −0.19, −0.1, and −0.4 °C, respectively. For the long-term daily mean LST, model RMSEs for all five lakes are less than 1 °C.

7. Conclusions and discussion

For the first time, an unstructured FVCOM was applied to all five Great Lakes simultaneously to simulate lake circulation and thermal structure. The purposes are two folds: (1) this model will serve as a backbone platform to be coupled to a regional atmospheric model for regional climate and downscaling studies, and (2) this model will be transferred into an operational model in the Great Lakes. The model was run under the NARR's 3-hourly forcing for the period 1993–2008. The model results are analyzed with a comparison to the observations and previous theory and modeling works. The main results are as follows.

- (1) Maps of climatological circulation for all five Great lakes are constructed using the simulations from 1993 to 2008. This climatology can be used as one of references for the general circulation in the Great Lakes due to the lack of continuous spatial and temporal observations. Most of the circulation pattern is in agreement with the observations, such as two-gyre type circulation in Lakes Ontario and Erie and one large-scale cyclonic circulation in Lakes Superior, Michigan, and Huron during winter; cyclonic circulation in Lakes Superior, Huron and Ontario during summer. While some features are controversial. For example, the model shows an anticyclonic gyre in the south basin of Lake Michigan, whose existence needs more work to verify. It is most likely caused by anticyclonic vorticity in the surface winds. The observed circulation patterns can only be considered as general representation of currents patterns and not climatology (Schertzer, 2003). Seasonal circulation in the Great Lakes has obvious interannual variability, which has rarely been studied due to insufficient data (Beletsky et al., 1999b). Some features of lake circulation appear to be rather stable, while others exhibit significant variability. Thus, differences between the modeled climatology of seasonal circulation and the observed circulation pattern in an individual year are expected, and some of them may be attributed to the interannual variability. Because of the lack of ice model, there are also potential inaccuracies of winter circulation patterns in Lakes Superior, Huron and Erie, which are usually heavily ice covered.
- (2) With the surface wind-wave mixing parameterization implemented to this FVCOM, the seasonal mixed-layer depths and sharp thermoclines in all five Great Lakes are significantly improved, compared to previous studies with no wind-wave mixing. The improvement was also reflected by the consistently well comparison in surface lake temperature between the satellite and buoy's data and the model. The model also reasonably reproduces inverse temperature

Table 2

Statistics of the model skill of lake surface temperature for each lake in 1998.^a

	Superior	Michigan	Huron	Erie	Ontario
Mean_obs. (°C)	7.94	10.96	9.79	12.36	10.95
Mean_model (°C)	7.91	10.24	9.87	11.22	10.38
Bias (°C)	−0.03	−0.72	0.08	−1.14	−0.57
MBD (%)	−0.34	−6.49	0.84	−9.19	−5.16
RMSE (°C)	1.28	0.81	0.86	1.88	1.14

^a Bias is model temperature minus observed temperature.

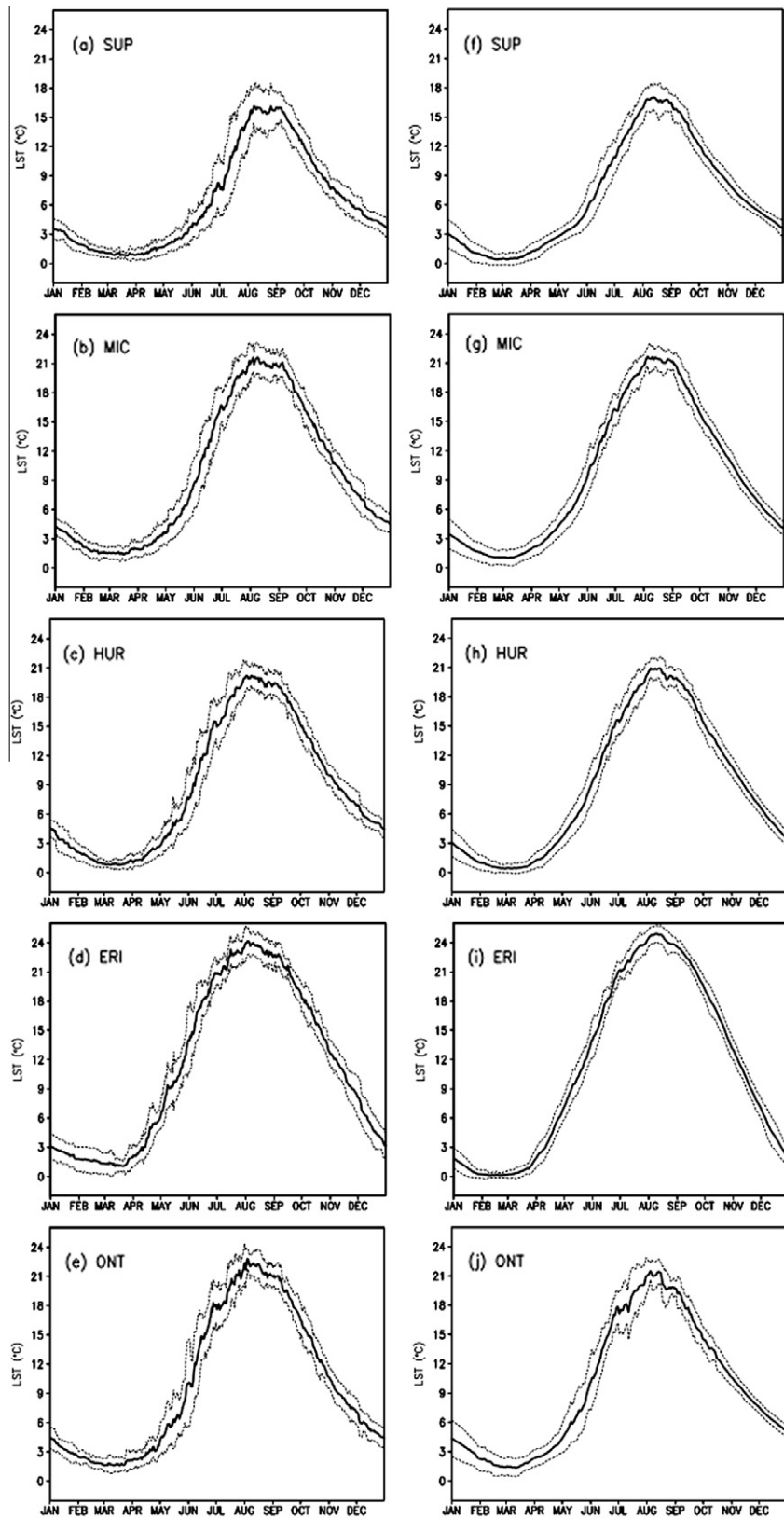


Fig. 26. Satellite observed (left column a–e) and Modeled (right column f–j) long term daily mean lake-wide averaged surface temperature (solid line) and standard deviation (dashed line) for each lake.

stratification during winter, and two seasonal overturns in autumn and spring, with the lower lakes leading the upper lakes by about 1–2 months.

- (3) The Great Lakes experienced significant interannual variability in terms of current speed, mixed-layer depth, and thermal structure in response to the changes in air

Table 3Statistics of the model skill of lake surface temperature for each lake for climatology.^a

	Superior	Michigan	Huron	Erie	Ontario
Mean_obs. (°C)	6.57	9.75	8.93	11.38	10.05
Mean_model (°C)	6.99	9.56	8.97	11.48	9.65
Bias (°C)	0.42	-0.19	0.04	0.10	-0.4
MBD (%)	6.4	-2.0	0.46	-1.8	-3.9
RMSE (°C)	0.95	0.47	0.67	0.83	0.92

^a Bias is model temperature minus observed temperature.

temperature and wind speed. Domain-average current speed increased as wind speed increased. Furthermore, it is found that more wind energy was input to deeper water over the period 1993–2008; similarly, more heat penetrated into deeper water as strong wind enhanced deeper mixing, leading to deeper convection in the deep-water lakes.

Acknowledgments

NARR Reanalysis data was provided by the NOAA/OAR/ESRL PSD, Boulder, Colorado, USA, from their Web site at <http://www.cdc.noaa.gov/>. This study was supported by grants from National Research Council Research association Fellowship and NOAA GLERL and EPA/NOAA Great Lakes Restoration Initiative. We thank Dr. Dmitry Beletsky for his valuable suggestions. We appreciate Cathy Darnell for her editorial assistance. We thank two anonymous reviewers for comments on an earlier version of the manuscript. This is GLERL Contribution No. 1649.

References

- Allender, J.H., Saylor, J.H., 1979. Model and observed circulation throughout the annual temperature cycle of Lake Michigan. *J. Phys. Oceanogr.* 9, 573–579.
- Ayers, J.C., Chandler, D.C., Lauff, G.H., Powers, C.F., Henson, E.B., 1958. Currents and Water Masses of Lake Michigan. Great Lakes Research Institute, University of Michigan, Publication No. 3.
- Ayers, J.C., Anderson, D.V., Chandler, D.C., Lauff, G.H., 1956. Currents and Water Masses of Lake Huron, Great Lakes Research Institute, University of Michigan, Technical Paper No. 1, p. 100.
- Bai, X., Wang, J., Sellinger, C.E., Clites, A.H., Assel, R.A., 2012. Interannual variability of Great Lakes ice cover and its relationship to NAO and ENSO. *J. Geophys. Res.* 117, C0002. <http://dx.doi.org/10.1029/2010JC006932>.
- Bai, X., Wang, J., Liu, Q., Wang, D., Liu, Y., 2011. Severe ice conditions in the Bohai Sea, China and mild ice conditions in the Great Lakes during the 2009/2010 winter: links to El Niño and a strong negative Arctic oscillation. *J. Appl. Meteorol. Climatol.* 50, 1922–1935. <http://dx.doi.org/10.1175/2011JAMC2675.1>.
- Beletsky, D., Schwab, D.J., 2008. Climatological circulation in Lake Michigan. *Geophys. Res. Lett.* 35, L21604. <http://dx.doi.org/10.1029/2008GL035773>.
- Beletsky, D., Schwab, D.J., 2001. Modeling circulation and thermal structure in Lake Michigan: annual cycle and interannual variability. *J. Geophys. Res.* 106 (C9), 19745–19771.
- Beletsky, D., Schwab, D.J., McCormick, M.J., 2006. Modeling the 1998–2003 summer circulation and thermal structure in Lake Michigan. *J. Geophys. Res.* 111, C10010. <http://dx.doi.org/10.1029/2005JC003222>.
- Beletsky, D., Lee, K.K., Schwab, D.J., 1999a. Large scale circulation. In: Lam, D.C.L., Schertzer, W.M. (Eds.), *Potential Climate Change Effects on Great Lakes Hydrodynamics and Water Quality*. American Society of Civil Engineers, Reston, VA, pp. 4.1–4.42.
- Beletsky, D., Hawley, N., Rao, Y.R., Vanderploeg, H.A., Beletsky, R., Schwab, D.J., Ruberg, S.A., 2012. Summer thermal structure and anticyclonic circulation of Lake Erie. *Geophys. Res. Lett.* 39, L06605. <http://dx.doi.org/10.1029/2012GL051002>.
- Beletsky, D., Saylor, S.H., Schwab, D.J., 1999b. Mean circulation in the Great Lakes. *J. Great Lakes Res.* 25, 78–93.
- Bennett, J.R., 1974. On the dynamics of wind-driven lake currents. *J. Phys. Oceanogr.* 4, 400–414.
- Bennington, V., McKinley, G.A., Kimura, N., Wu, C.H., 2010. General circulation of Lake Superior: mean, variability, and trends from 1979 to 2006. *J. Geophys. Res.* 115, C12015. <http://dx.doi.org/10.1029/2010JC00626>.
- Casey, D.J., Fisher, W., Kleveno, C.O., 1966. Lake Ontario environmental summary—1965, Report No. EPA-902/9-73-002, US Environmental Protection Agency, Region II, Rochester, NY.
- Chen, C., Beardsley, R.C., Cowles, G., 2006. An unstructured grid, finite-volume coastal ocean model (FVCOM) system. *Oceanography* 19 (1), 78–89, Special Issue entitled “Advance in Computational Oceanography”.
- Chen, C., Liu, H., Beardsley, R.C., 2003. An unstructured, finite-volume, three-dimensional, primitive equation ocean model: application to coastal ocean and estuaries. *J. Atmos. Oceanic Technol.* 20, 159–186.
- Chen, C., Zhu, J., Ralph, E., Green, S.A., Wells Budd, J., Zhang, F.Y., 2001. Prognostic modeling studies of the Keweenaw current in Lake Superior. Part I: Formation and evolution. *J. Phys. Oceanogr.* 31, 379–395.
- Craig, P.D., Banner, M.L., 1994. Modeling wave-enhanced turbulence in the ocean surface layer. *J. Phys. Oceanogr.* 24, 2546–2559.
- Gottlieb, E.S., Saylor, J.H., Miller, G.S., 1989. Currents and temperatures observed in lake michigan from June 1982 to July 1983. NOAA Technical Memorandum, GLERL-71, Great Lakes Environmental Research Laboratory Ann Arbor, Michigan.
- Hamblin, P.F., 1971. Circulation and water movement in Lake Erie, Inland Waters Branch Scientific Series No. 7. Canada Department of Energy, Mines, and Resources, Ottawa, Ont., p. 49.
- Harrington, M.W., 1895. Surface current of the Great Lakes, as deduced from the movements of bottle papers during the seasons of 1892, 1893, and 1894. US Weather Bureau Bull. B., p. 20.
- Hill, D.K., Magnuson, J.J., 1990. Potential effects of global climate warming on the growth and prey consumption of Great Lakes fish. *Trans. Am. Fish. Soc.* 119, 265–275.
- Hu, H., Wang, J., 2010. Modeling effects of tidal and wave mixing on circulation and thermohaline structures in the Bering Sea: process studies. *J. Geophys. Res.* 115, C01006. <http://dx.doi.org/10.1029/2008JC005175>.
- Huang, A., Rao, Y.R., Lu, Y., Zhao, J., 2010. Hydrodynamic modeling of Lake Ontario: an intercomparison of three models. *J. Geophys. Res.* 115, C12076. <http://dx.doi.org/10.1029/2010JC006269>.
- Huang, J.C.K., Sloss, P.W., 1981. Simulation and verification of Lake Ontario's mean state. *J. Phys. Oceanogr.* 11, 1548–1566.
- Jerlov, N.G., 1968. Optical Oceanography. Elsevier, p. 194.
- Jerlov, N.G., 1976. Marine Optics. Elsevier Sci. Pub. Co., Amsterdam, p. 231.
- Large, W.G., Pond, S., 1982. Sensible and latent heat flux measurements over the ocean. *J. Phys. Oceanogr.* 12, 464–482.
- León, L.F., Imberger, J., Smith, R.E.H., Hecky, R.E., Lam, D.C.L., Schertzer, W.M., 2005. Modeling as a tool for nutrient management in Lake Erie: a hydrodynamics study. *J. Great Lakes Res.* 31 (Suppl. 2), 309–318.
- Lien, S.L., Hoops, J.A., 1978. Wind-driven, steady flows in Lake Superior. *Limnol. Oceanogr.* 23 (1), 91–103.
- Luo, L., Wang, J., Schwab, D.J., Vanderploeg, H.A., Leshkevich, G.A., Bai, X., Hu, H., Wang, D., 2012. Simulating the 1998 spring bloom in Lake Michigan using a coupled physical-biological model. *Journal of Geophysical Research* 117 (C10011), 14. <http://dx.doi.org/10.1029/2012JC008216>.
- McCormick, M., Pazdalski, J.D., 1993. Monitoring midlake water temperature in southern Lake Michigan for climate change studies. *Climatic change* 25 (2), 119–125. <http://dx.doi.org/10.1007/BF01661201>.
- Mellor, G.L., 2001. One-dimensional, ocean surface layer modeling, a problem and a solution. *J. Phys. Oceanogr.* 31 (3), 790–809.
- Mellor, G.L., Blumberg, A., 2004. Wave breaking and ocean surface thermal response. *J. Phys. Oceanogr.* 34, 693–698.
- Mellor, G.L., Yamada, T., 1982. Development of a turbulence closure model for geophysical fluid problems. *Rev. Geophys. Space Phys.* 20, 851–875.
- Mesinger, F., co-authors, 2006. North American Regional Reanalysis. *Bull. Am. Meteorol. Soc.* 87, 343–360. doi: <http://dx.doi.org/10.1175/BAMS-87-3-343>.
- Mortimer, C.H., 1987. Fifty years of physical investigations and related limnological studies on Lake Erie, 1928–1977. *J. Great Lakes Res.* 13, 407–435.
- Paulson, C.A., Simpson, J., 1977. Irradiance measurements in the upper ocean. *J. Phys. Oceanogr.* 7, 952–956.
- Petterssen, S., Calabrese, P.A., 1959. On some weather influences due to warming of the air by the great lakes in winter. *J. Meteor.* 16, 646–652.
- Pickett, R.L., 1977. The observed winter circulation of Lake Ontario. *J. Phys. Oceanogr.* 7, 152–156.
- Pickett, R.L., 1980. Observed and predicted Great Lakes winter circulations. *J. Phys. Oceanogr.* 10, 1140–1145.
- Pickett, R.L., Rao, D.B., 1976. One- and two-gyre circulations in homogeneous lakes. *IFYGL Bulletin*, 19, NOAA, Rockville, Md., p. 101.
- Pickett, R.L., Bermick, S., 1977. Observed resultant circulation of Lake Ontario. *Limnol. Oceanogr.* 22, 1071–1076.
- Prakash, S., Atkinson, J.F., Green, M.L., 2007. A semi-Lagrangian study of circulation and transport in Lake Ontario. *J. Great Lakes Res.* 33 (4), 774–790. <http://dx.doi.org/10.3394/0380-1330>.
- Qiao, F., Yuan, Y., Yang, Y., Zheng, Q., Xia, C., Ma, J., 2004. Wave-induced mixing in the upper ocean: distribution and application to a global ocean circulation model. *Geophys. Res. Lett.* 31, L11303. <http://dx.doi.org/10.1029/2004GL019824>.
- Rao, D.B., Murty, T.S., 1970. Calculation of the steady state circulations in Lake Ontario. *Arch. Meteorol. Geophys. Bioklimatol. Ser. A* 19, 195–210.
- Rodgers, G.K., 1966. The thermal bar in Lake Ontario, spring 1965 and winter 1965–1966. *Proc. Ninth Conf. Great Lakes Res.*, 15. Great Lakes Res. Div. Publ., University of Michigan, pp. 369–374.
- Rodgers, G.K., Anderson, D.V., 1963. The thermal structure of Lake Ontario. *Proc. Sixth Conf. Great Lakes Res.*, 10. Great Lakes Res. Div. Publ., University of Michigan, pp. 59–69.
- Saylor, J., Bennett, J.R., Boyce, F.M., Liu, P.C., Murthy, C.R., Pickett, R.L., Simons, T.J., 1981. Water movements. In: Aubert, E.J., Richards, T.L. (Eds.), *IFYGL – The International Field Year for the Great Lakes*. Natl. Oceanic and Atmos. Admin. Great Lakes Env. Res. Lab., Ann Arbor, Michigan, pp. 247–324.

- Saylor, J.H., Miller, G.S., 1983. Investigation of the currents and density structure of Lake Erie. NOAA Technical Memorandum ERL GLERL-49, Great Lakes Environmental Research Laboratory Ann Arbor, Michigan.
- Saylor, J.H., Miller, G.S., 1987. Studies of large-scale currents in Lake Erie, 1979–1980. *J. Great Lakes Res.* 13, 487–514.
- Saylor, J., Miller, G., 1976. Winter circulations in Lake Huron, NOAA Tech. Memo. ERL-GLERL 15, US Dep. of Commerce, Boulder, Colo.
- Saylor, J., Miller, G., 1979. Lake Huron winter circulation. *J. Geophys. Res.* 84 (C6), 3237–3252.
- Schertzer, W.M., 2003. Physical limnology and hydrometeorological characteristics of Lake Ontario with consideration of climate impacts. In: Munawar, (Ed.), State of Lake Ontario: Past, Present and Future. Ecovision World Monography Series. Aquatic Ecosystem Health & Management Society, 664pp.
- Schwab, D.J., 1992. Hydrodynamics modeling in the Great from 1950 to 1990 and prospects for the future. In: Gobas, F., McCorquodale, J. (Eds.), Chemical Dynamics in Freshwater Ecosystems. Lewis Publishers, Boca Raton, FL, pp. 41–62.
- Schwab, D.J., Beletsky, D., 2003. Relative effects of wind stress curl, topography, and stratification on large-scale circulation in Lake Michigan. *J. Geophys. Res.* 108 (C2), 3044. <http://dx.doi.org/10.1029/2001JC001066>.
- Schwab, D.J., Bedford, K.W., 1999 (The Great Lakes Forecasting System). In: Mooers, C.N.K. (Ed.), Coastal Ocean Prediction, Coastal and Estuarine Studies, 56. American Geophysical Union, Washington, DC, pp. 157–173.
- Schwab, D.J., O'Connor, W.P., Mellor, G.L., 1995. On the net cyclonic circulation in large stratified lakes. *J. Phys. Oceanogr.* 25, 1516–1520.
- Schwab, D.J., Beletsky, D., DePinto, J., Dolan, D.M., 2009. A hydrodynamic approach to modeling phosphorous distribution in Lake Erie. *J. Great Lakes Res.* 35 (1), 50–60. <http://dx.doi.org/10.1016/j.jglr.2008.09.003>.
- Schwab, D.J., Leshkevich, G.A., Muhr, G.C., 1992. Satellite measurements of surface water temperature in the Great Lakes: Great Lakes Coast Watch. *J. Great Lakes Res.* 18 (2), 247–258.
- Sheng, J.Y., Rao, Y.R., 2006. Circulation and thermal structure in Lake Huron and Georgian Bay: application of a nested-grid hydrodynamic model. *Cont. Shelf Res.* 26 (12–13), 1496–1518. <http://dx.doi.org/10.1016/j.csr.2006.01.019>.
- Simons, T.J., 1971. Development of numerical models of Lake Ontario. In: Proc. 14th Conf. Great Lakes Res., Intern. Assoc. Great Lakes Res., Ann Arbor, Mich., pp. 654–669.
- Simons, T.J., Murthy, C.R., Campbell, J.E., 1985. Winter circulation in Lake Ontario. *J. Great Lakes Res.* 11, 423–433.
- Sloss, P.W., Saylor, J.H., 1976. Large-scale current measurements in Lake Superior. NOAA Tech. Rep. ERL-GLERL 8.
- Sloss, P.W., Saylor, J.H., 1975. Measurements of current flow during summer in Lake Huron. NOAA Tech. Rep. ERL 353-GLERL 5, US Dep. of Commerce, Boulder, Colo.
- Smagorinsky, J., 1963. General circulation experiments with the primitive equations. *Mon. Weather Rev.* 91, 99–164.
- Wang, J., Hu, H., Schwab, D.J., Leshkevich, G.A., Beletsky, D., Hawley, N., Clites, A.H., 2010. Development of the Great Lakes ice circulation model (GLIM): application to Lake Erie in 2003–2004. *J. Great Lakes Res.* 36, 425–436.
- Wyrtki, K., 1965. The average annual heat balance of the North Pacific ocean and its relation to ocean circulation. *J. Geophys. Res.* 70 (18), 4547–4559.
- Yuan, Y., Qiao, F., Hua, F., Wan, Z., 1999. The development of a coastal circulation numerical model. 1. Wave-induced mixing and wave-current interaction. *J. Hydron. Ser. A* 14, 1–8 (in Chinese with English abstract).
- Yuan, Y., Pan, Z., Sun, L., 1991. LAGDF-WAM numerical wave model. *Acta Oceanol. Sin.* 10, 483–488.
- Zhu, J., Chen, C., Ralph, E., Green, S.A., Budd, J.W., Zhang, F.Y., 2001. Prognostic modeling studies of the Keweenaw current in Lake Superior. Part II: Simulation. *J. Phys. Oceanogr.* 31, 396–410.